NASA Technical Memorandum 106281
AIAA–93–1825

A Laboratory Model of a Hydrogen/Oxygen Engine for Combustion and Nozzle Studies

Sybil Huang Morren
Lewis Research Center
Cleveland, Ohio

Roger M. Myers
Sverdrup Technology, Inc.
Lewis Research Center Group
Brook Park, Ohio

Stephen E. Benko
Lewis Research Center
Cleveland, Ohio

Lynn A. Arrington
Sverdrup Technology, Inc.
Lewis Research Center Group
Brook Park, Ohio

and

Brian D. Reed
Lewis Research Center
Cleveland, Ohio

Prepared for the
29th Joint Propulsion Conference and Exhibit
sponsored by the AIAA, SAE, ASME, and ASEE
Monterey, California, June 28–30, 1993

NASA

A Laboratory Model of a Hydrogen/Oxygen Engine for Combustion and Nozzle Studies

Sybil H. Morren
National Aeronautics and Space Administration
Lewis Research Center
Cleveland, Ohio 44135

Roger M. Myers
Sverdrup Technology, Inc.
Lewis Research Center Group
Brook Park, Ohio 44142

Stephen E. Benko
National Aeronautics and Space Administration
Lewis Research Center
Cleveland, Ohio 44135

Lynn A. Arrington
Sverdrup Technology, Inc.
Lewis Research Center Group
Brook Park, Ohio 44142

and

Brian D. Reed
National Aeronautics and Space Administration
Lewis Research Center
Cleveland, Ohio 44135

Abstract

A small laboratory diagnostic thruster was developed to augment present low thrust chemical rocket optical and heat flux diagnostics at the NASA Lewis Research Center. The objective of this work was to evaluate approaches for the use of temperature and pressure sensors for the investigation of low thrust rocket flow fields. The nominal engine thrust was 110 N. Tests were performed at chamber pressures of about 255 kPa, 370 kPa, and 500 kPa with oxidizer to fuel mixture ratios between 4.0 and 8.0. Two gaseous hydrogen/gaseous oxygen injector designs were tested with 60% and 75% fuel film cooling. The thruster and instrumentation designs were proven to be effective via hot fire testing. The thruster diagnostics provided inner wall temperature and static pressure measurements which were compared to the thruster global performance data. For several operating conditions, the performance data exhibited unexpected trends which were correlated with changes in the axial wall temperature distribution. Azimuthal temperature distributions were found to be a function of operating conditions and hardware configuration. The static pressure profiles showed that no severe pressure gradients were present in the rocket. The results indicated that small differences in injector design can result in dramatically different thruster performance and wall temperature behavior, but that these injector effects may be overshadowed by operating at a high fuel film cooling rate.

Introduction

Low thrust propulsion systems are on-board virtually every launch and space vehicle, satellite, and spacecraft, and perform such duties as apogee insertion, attitude control, docking, and separation. Changes in spacecraft performance, lifetime, reliability, and contamination requirements are forcing continued development of low thrust chemical engine technology . To address these technology requirements, improved predictive tools, specifically designed for small rockets, are essential.

Current design tools do not fully address the complex fluid and combustion processes of small rockets. Most high thrust rocket models assume the rocket behaves as an inviscid core with a thin boundary layer[1,2]. For relatively large rockets, these are good assumptions and result in accurate predictions of rocket performance. However, for small rockets with thrust levels below 4500 N mixing in the boundary and shear layers and combustion effects are more dominant phenomena. Therefore, severe thermal, velocity, and species gradients can exist in small rockets which must be included in the design process.

Large engine codes have been used for modeling small rockets with mixed results. Richter and Price[3] found that the predictions for small hydrogen/oxygen rockets did not compare well with experimental results. Smith et al.[4] tested a high area ratio nozzle engine which had a relatively thick boundary layer flow field and also found that the Joint Army, Navy, NASA, Air Force (JANNAF) rocket engine performance prediction code[5] used in conjunction with the reference code, Two Dimensional Kinetics (TDK) program[6], did not agree with experimental results. Kehtarnavaz and Coats[2] compared TDK[6] and various other codes for modeling thick boundary layer flow field rockets and found the thin boundary layer assumptions used were inadequate for modeling the flows. Although more comprehensive codes using Navier-Stokes analyses are being developed[7,8,9], there is currently a lack of local flow field data to use for code development and verification. This deficiency of experimental data is largely due the lack of a sustained program to gather and analyze local flow field data for small rockets.

This paper describes the design and preliminary test results of a small laboratory thruster developed to augment present optical[10,11,12] and heat flux[13] diagnostics for low thrust chemical rockets at NASA Lewis Research Center. The thruster provides simple measurements of interior wall temperatures and static pressures for the purpose of evaluating rocket flow fields. Previous works have also used simple diagnostic

techniques to evaluate rocket flow fields. Schoenman and Block[14] hot fire tested several engines instrumented with axial and azimuthal thermocouples which were brazed or welded into place. Back et al.[15] used translating pitot tube and thermocouple probes to study the boundary layer and heat transfer in a conical nozzle running with pressurized, heated air. Richter and Price[3] tested a low thrust gaseous hydrogen/gaseous oxygen, regeneratively cooled thruster and measured chamber exterior wall temperatures. Kacynski et al.[16] conducted a heat flux analysis of a high area ratio nozzle and measured nozzle exterior (backside) wall temperatures with spot welded thermocouples. Rousar and Ewen[17] had a fairly comprehensive temperature measurements system with axial and azimuthal temperature measurements for a thin walled chamber which was cooled only by the internal film cooling.

Although simple diagnostic techniques were employed in the past, most engine diagnostics were welded or brazed into place, and azimuthal temperature measurements were often limited to a few axial locations. The water-cooled gaseous hydrogen/oxygen laboratory thruster discussed in this paper employed instrumentation designed for ease of maintenance and repair. The instrumentation and thruster joint sealing techniques required to provide maximum flexibility for instrumentation replacement are described in this paper. The thruster provided axial pressure and axial and azimuthal temperature distributions in the combustor, throat, and nozzle sections. Testing was conducted with two injector designs which employed fuel film cooling (FFC) to protect the chamber wall. Comparisons of the global performance data to local temperature and pressure measurements were made. The azimuthal performance of the injectors and effects due to differences in injector design and fuel film cooling rates were also investigated.

Apparatus and Procedure

Chamber

The thruster liner and outer housing were fabricated from Oxygen Free High Conductivity (OFHC) copper. The thruster was designed to deliver 110 N thrust at a nominal chamber pressure (P_c) of 500 kPa. The overall thruster length was 20.3 cm with a 2.54 cm diameter chamber, a 1.27 cm diameter throat, and a nozzle expansion area ratio of 33:1. The nozzle was conical with a nominal 19° half angle. A conical nozzle was used instead of an optimized bell nozzle contour to simplify the thruster fabrication.

The laboratory thruster used an instrumentation procedure developed to accommodate the water cooling design. Instrumentation details are shown in Figure 1. The thruster was water cooled using milled channels on the back side of the liner as shown in Figure 1(a). The channels were 0.032 cm high by 0.032 cm wide. The wall thickness from the bottom of the channels to the hot gas side surface was also 0.032 cm. There were 11 channels in the combustion chamber and throat section which bifurcated into 22 channels in the nozzle. A typical bifurcated channel is illustrated in Figure 1(a). The channel bifurcation ensured uniform cooling of the large nozzle surface area. A clam shell type outer housing slid over the liner and was joined to the liner at the water inlet and outlet manifolds shown in Figure 2, and along the two axial seams where the outer housing was split. The clam shell housing style was chosen because it allowed the chamber, throat, and nozzle to be fabricated in one piece. The thruster joints were soldered using a high temperature solder. Brazing was not desirable because the thermal cycle required to braze would have degraded the structural integrity of the copper. Welding was also not feasible due to the high conductivity of OFHC copper. The solder joints were reinforced by bolts at the water manifold flanges. While the lower temperature limit of the solder joints were a concern prior to a hot fire testing, there were no signs of water leakage after the completion of the tests.

Sensors

The laboratory thruster had 30 thermocouples located in 4 rows spanning the combustor and nozzle sections. The axial and azimuthal locations of the thermocouples are identified in Figure 2. Typical thermocouple rows and the ports are shown in Figures 1(a) and 1(b), respectively. As seen in Figure 1(b), the instrumentation ports were located in the channel lands, which were located between cooling channels. While the exterior liner wall mated tightly to the interior wall of the outer housing, the exterior liner wall (channel lands) were not bonded to the outer jacket. Therefore, a water seal was required in the instrumentation ports. The chromel-alumel thermocouples were nominally 0.80 mm in diameter. The 0.85 mm diameter thermocouple ports were drilled to within 0.76 mm of the hot gas side surface. The small size of the instrumentation ports made it difficult to verify the port tolerances. Therefore, thermocouple measurements were carefully assessed to ensure that temperature anomalies were not due to thermocouple placement.

Figure 1(c) is an exploded view of a typical thermocouple installation. The graphite foil washer sealed water on the back side of the liner. Graphite foil material was used because of its high temperature limit. The fluorinated polymer washer was used to prevent water from leaking through the backside of the outer housing. The fluorinated polymer seal for the liner fitting sealed the water which flows between the liner fitting and the outer housing fitting. The seal cap and fluorinated polymer seal were drilled through to allow insertion of a liner fitting. The fittings were installed after the thruster outer housing and liner were joined. The liner fitting and graphite foil washer were installed first. A pipe sealing compound mixed with a fluorinated polymer and graphite was applied to the threads to provide added sealing capability. The sealing cap and outer housing fitting with the fluorinated polymer washer slid over the liner fitting. The thermocouple was then inserted through the fittings and secured in place by the thermocouple spring.

The static pressure ports used the same instrumentation ports and instrumentation fittings as the thermocouples. The pressure ports were drilled through the liner wall and were 0.85 mm in diameter. The liner fitting shown in Figure 1(c) was used as the pressure sensing line and connected to tubing which terminated at the pressure transducers. The pressure transducers were located outside of the vacuum tank. The pressure measurements were monitored carefully to ensure steady state pressure conditions were achieved during testing.

The instrumentation fabrication and assembly techniques greatly simplified the replacement of faulty sensors. The replacement of a damaged thermocouple only required the unfastening of the spring and insertion of a new thermocouple. In case of a water leak, repair of the sealing surfaces simply required unscrewing the fittings and inserting new washers. All of the instrumentation was easily replaced, and repairs were made *in situ* without removal of the engine from the test stand.

Injectors

Two platelet injectors designed by Aerojet GenCorp Propulsion Division[18] were used to verify operation of the laboratory thruster. The injectors were part of a Space Station Freedom low-thrust, gaseous hydrogen/gaseous oxygen rocket technology program and were originally designed to be tested with a regeneratively cooled thruster.[18] The two injectors, designated SN. 02 and SN. 03, were nearly identical designs. Injector SN. 02 was modified in-house to improve ignition reliability by enlarging the gap at the base

which prevented the spark plug from arcing at the base. However, in a study by Arrington and Reed[19] using the modified SN. 02 injector, performance anomalies were observed. The unmodified injector SN. 03 was tested so that any performance, wall temperature, and pressure changes due to injector design could be identified.

The propellant flow paths for both injectors are shown in Figure 3. The oxygen entered through a platelet stack and was injected radially toward the spark plug, upstream of the spark plug tip. The hydrogen entered a fuel manifold within the injector/combustor cavity. Part of the hydrogen entered the platelet stack and was injected radially just downstream of the spark plug tip. The remaining hydrogen flowed down milled channels on the fuel film cooling sleeve. A fuel splitting washer, located against the flange of the fuel film cooling sleeve, determined the percentage of hydrogen which flowed down the sleeve. At the exit of the fuel film cooling sleeve, the chamber contained an oxidizer rich core of combustion gases surrounded by a hydrogen cooling film. Both platelet injectors were designed for fuel film cooling using 60% of the total fuel flow rate, a nominal chamber pressure (P_C) of 500 kPa, and a mixture ratio (MR) of 8.0. The injectors were also tested at fuel film cooling rates of 75% FFC by changing the fuel splitting washer to compare global and local changes due to fuel film cooling variation.

The core mixture ratios were above stoichiometric for every test condition, and cab be calculated as the overall mixture ratio divided by the quantity of one minus the fuel film cooling faction. Therefore, the core flow contained mixture ratios between MR of 10 and 20 with 60% FFC, and between MR of 16 and 32 with 75% FFC. All mixture ratios reported in this paper refer to the total fuel and oxidizer flows.

Test Facility

The testing was performed in the NASA Lewis Research Center RL-11 test cell. A schematic of the RL-11 is shown in Figure 4. The RL-11 test cell was capable of testing gaseous hydrogen/gaseous oxygen chemical rockets at thrust levels up to 220 N. The altitude capsule was a 0.9 m diameter and 1.8 m long tank. A two stage, air driven ejector system pumped the tank down to a soft vacuum of 1.4 kPa. During a hot fire test, the exhaust gases were fired into a water cooled diffuser. Downstream of the diffuser, the hot gases were cooled by a spray cart prior to entering the ejectors. A personal computer based data acquisition system received and displayed measured and calculated parameters

on display screens. Data were recorded on strip charts, FM tape, and floppy disks. An extensive discussion of the facility is found in Reference 20.

Results and Discussion

Chamber and Sensor Operations

The laboratory thruster diagnostics were used to assess different injectors and fuel film cooling rates through their effects upon wall temperature and static pressure profiles. After the completion of 396 hot fire tests, the thruster instrumentation proved to have good water sealing capability and good accessibility for *in situ* maintenance and repairs. Minimal water leakage was experienced, and water leak repairs were made in a matter of a few hours. Thermocouple replacements were accomplished in a few minutes. Also, wall temperature measurements showed no evidence of localized heating or distortion of the thruster. No leaks from the thruster liner and outer housing joints were detected. Because of the high water cooling flow rate of 0.693 kg/s, there was a concern that every test condition would be forced to the same wall temperature distribution. However, the test results proved that the thermocouples could detect temperature changes resulting from differences in injector and/or fuel film cooling rate. Another concern was that inaccuracies in thermocouple placement would introduce large measurement uncertainties. However, extensive testing revealed no biases in the wall temperature measurements, and the azimuthal temperature profile symmetry varied widely depending upon the test conditions and fuel film cooling rates. These results show that the anomalies of the azimuthal temperature profiles, discussed below, were due to real flow field effects.

Azimuthal Symmetry

Azimuthal symmetry is a key assumption in the modeling of rocket engine flow fields. Therefore, the degree of azimuthal symmetry in the flows must be determined to ensure an accurate rocket model. Azimuthal temperature profiles were measured as a function of operating conditions for the two injectors. Both injectors were tested with the chamber illustrated in Figures 1 and 2, and used the same fuel sleeve and fuel splitting washers. The only known difference between the two injectors was the small modification made

on SN. 02 described earlier, which was not anticipated to have effects upon the azimuthal symmetry. The azimuthal temperature distributions for both injectors, which are shown in Appendix A, showed clearly that the symmetry varied with test condition for both injectors. For a given test condition, the two injectors exhibited different azimuthal temperature patterns except at the high mixture ratio, 75% FFC tests, where both injectors displayed similar, azimuthally symmetric temperature profiles. The observed temperature profiles implied that small differences in injector designs may have large impacts on local flow field characteristics of small rockets. The variation of azimuthal symmetry with test conditions was an important finding which must be investigated further to support both the definition of manufacturing processes and the development of accurate rocket flow field models for low thrust chemical engines.

Although the azimuthal temperature profiles were not symmetric in most cases for either injector, the trends in the axial temperature distribution were similar for different azimuthal locations (thermocouple rows), and for specific thermocouples. In addition, the temperature measurements for a given operating condition were very reproducible from one test to another. This is illustrated in Appendix A by comparing results from typical thermocouple rows and single thermocouple locations. In order to simplify the presentation of the results, only data from thermocouple row B are used to display the behavior of the wall temperature measurements. Results for all other thermocouple rows were similar.

Performance Measurements

Thruster performance was measured to allow comparison with the local data. Figures 5 and 6 show the variations in characteristic velocity (C^*) and vacuum specific impulse (I_{sp_v}), respectively, with mixture ratio for the two thruster assemblies for FFC of 60% and 75%. The $C^*$and I_{sp_v} data were nearly identical, therefore only the I_{sp_v} results will be discussed below.

For 60% FFC, thruster assembly SN. 03 performed better than SN. 02 at lower mixture ratios as shown in Figure 6, but performance differences diminished above MR=5.0. I_{sp_v} decreased linearly with increasing mixture ratio for the SN. 03 thruster assembly. The SN. 02 thruster performance curve decreased monotonically with increasing MR, but was not linear. The performance deviated from that of injector SN. 03 for MR below 6.0.

For FFC=75% the I_{sp_v} data exhibited similar trends for both thruster assemblies. The FFC=75% performance data did not decrease monotonically. Between MR of 5.0 and 6.0 the I_{sp_v} values increased locally near MR of 6.0. The SN. 03 thruster exhibited lower I_{sp_v} values than the SN. 02 thruster for all MRs tested.

The performance changes with increasing MR for both the SN. 02 and SN. 03 thruster assemblies with 60% and 75% FFC fell into three categories. The first was the linear decrease in I_{sp_v} of the SN. 03 thruster with 60% FFC. This behavior was similar to the trends observed in a previous study by Reed et al.[21] The second category was the slight deviation from the linear profile exhibited by the SN. 02 thruster assembly with 60% FFC, and the third was the highly non-monotonic behavior of the two thruster assemblies with 75% FFC. This substantial variation in thruster performance behavior with changing MR led to a detailed examination of wall temperature distribution behavior.

Temperature Measurements

The axial temperature distributions for mixture ratios between 4 and 8 are shown in Figures 7 through 10. The thruster injector exit plane was at -3.81 cm and the throat was located at 0.0 cm. Figure 7 shows the axial temperature distributions for the SN.03 thruster assembly with 60% FFC. All the temperature profiles in Figure 7 followed a similar axial distribution pattern. The temperature sensitivity to MR was evident only in the combustor and throat sections. As shown in Figure 11, the temperature in the converging section (location B3) of the SN.03 thruster assembly generally decreased with MR. In the nozzle section the temperature variation disappeared.

The axial temperature distributions for the SN. 02 thruster assembly with 60% FFC (Figure 8) exhibited similar temperature profiles to those of Figure 7 for MR's above 6.0. However, for the lower MR tests the temperature distribution changed, resulting in lower wall temperatures than those obtained with MR above 6.0. The temperature profiles in Figure 8 exhibited much greater sensitivity to MR than was observed in Figure 7. The disparity in wall temperature was pronounced in the combustor and throat sections and was sustained in the nozzle section in contrast to the data in Figure 7. The temperature generally increased (Figure 11) with increasing MR, in contrast to the SN. 03, FFC 60% FFC results with decreased monotonically.

Figures 9 and 10 show the axial temperature profiles from the 75% FFC tests for the SN. 03 and SN. 02 thruster assemblies, respectively. The two thruster assemblies exhibited nearly identical temperature profiles. The shape of the profiles were similar to those of Figure 7. However, for the 75% FFC tests wall temperatures decreased drastically for MR below 6.0. The sensitivity to MR appears to have been sustained throughout the nozzle in the form of two distinct groupings of temperature profiles. For 75% FFC, both thruster assemblies exhibited similar temperature variations with MR (Figures 11).

Static Pressure Measurements

The static pressure distribution measurements for both injectors are shown in Figures 12 and 13. All the static pressure profiles were similar, and gave no indication of shocks or boundary layer separation. This result indicates that the temperature trends were dominated by mixing and/or shear layer interactions particular to injector design and fuel film cooling rates, and did not result from pressure gradients in the flow.

Low Chamber Pressure Results

Thus far, the results discussed have been restricted to comparisons of injector designs tested under two FFC rates with the laboratory thruster at the design chamber pressure of nominally 500 kPa. Injector SN. 02 underwent additional testing at off-design chamber pressures of nominally 255 and 370 kPa for the purpose of testing the thruster diagnostics at the lower P_c conditions. Typical I_{sp_v} performance data at the lower chamber pressures for 60% and 75% FFC are shown in Figure 14. The performance curves showed large non-monotonic behavior near a mixture ratio of 6.0 at 75% FFC. The trends for the 60% FFC tests showed only a slight non-monotonic behavior near a MR of 8.0 at P_c of 255 and 370 kPa. The corresponding temperature profiles shown in Figure 15 showed changes at the same operating conditions at which performance changes occurred. Temperatures increased significantly near MR of 6.0 for 75% FFC tests. For the 60% FFC tests, a significant temperature increase was observed between MR of 7.0 and 8.0 which corresponded to the non-monotonic behavior seen in Figure 14 near MR of 8.0. These low chamber pressure tests indicated that the diagnostic measurements continued to produce trends which support the global performance data at low chamber pressure conditions.

Comparison of Global and Local Data

The performance data of Figure 6 obtained from the SN. 03 thruster assembly with 60% FFC exhibited a nearly linear decreasing trend with increasing MR. The corresponding temperature profiles are shown in Figure 7. All the profiles of Figure 7 displayed the same axial temperature distribution, with a small decrease in wall temperature along the length of the combustion chamber, a large increase in the converging section, a maximum temperature near the throat, and a dramatic decrease in temperature along the length of the nozzle.

The performance measurements of Figure 6 for the SN. 02 thruster assembly with 60% FFC displayed monotonic, but non-linear characteristics. In general the performance was lower than that of the SN. 03 thruster. In Figure 8, a steep drop in wall temperature was observed with the SN. 02 thruster at 60% FFC for MR below 6.0 which corresponded to a decrease in performance relative to the performance of the SN. 03 thruster assembly. The temperature behavior of the SN. 02 thruster assembly for MR above 6.0 in Figure 8 was similar to that of the SN. 03 thruster shown in Figure 7. However, the profiles which represent conditions below MR of 6.0 showed an increase in wall temperature along the length of the combustion chamber. This contrasted to the decrease in wall temperature observed for thruster assembly SN. 03.

The I_{sp_v} data for both thruster assemblies with 75% FFC exhibited dramatic deviations from the nearly linear trend of the SN. 03 thruster assembly with 60% FFC for MR below 6.0. The temperature profiles at 75% FFC for the two thruster assemblies are shown in Figures 9 and 10. The temperature profile shapes were similar to those of Figure 7 for MR above 6.0. However, for tests with MR below 6.0 there was a significant decrease in wall temperature. In addition, the temperatures along the combustor section did not decrease as seen in Figure 7, but remained constant at MR conditions below 6.0. The large decrease in wall temperature seen in Figures 9 and 10 at MR below 6.0 correlated well with the pronounced performance deviations from the trends of both thruster assemblies SN. 03 and SN. 02 at 75% FFC.

A close examination of Figures 5 through 10 showed that changes in performance behavior were strongly correlated with changes in the behavior of the wall temperature distribution. Significant reduction in wall temperatures consistently occurred below MR of 6.0 for all tests conditions except for the SN. 03 thruster assembly with 60% FFC. The

performance curves and temperature profiles indicated that the SN. 02 and SN. 03 thruster assemblies operated differently for the same test conditions with 60% FFC. The significant differences in injector performance suggest that small differences in injector configuration can result in significantly different performance characteristics. However, these differences can be overshadowed by operating at extreme levels of FFC, as is evidenced by the similarity of the thruster behavior for cases using 75% FFC.

Summary

A laboratory model gaseous hydrogen/oxygen thruster was developed as a diagnostic tool for investigating low thrust rocket flow fields. The thruster fabrication and diagnostic techniques were proven effective via hot fire testing. Thruster performance and wall temperature and static pressure distributions were measured for two injectors as a function of both mixture ratio and fuel film cooling rate. The two injectors were identical in design with the single known exception of a small modification in the upstream region of one of the injectors. Test operating conditions included 60% and 75% fuel film cooling rates, nominal chamber pressures of 255 kPa, 370 kPa, and 500 kPa, and oxidizer to fuel ratios between 4.0 and 8.0.

The thruster and diagnostics fabrication and assembly procedures proved to allow easy and fast repair of all instrumentation as required to ensure accurate temperature and pressure measurements. Only minor water leaks and transducer failures were encountered which were rapidly repaired. The instrumented thruster sustained hundreds of hot fire tests with only minor maintenance.

The thruster diagnostics were shown to be a practical tool for investigating small rocket flow fields, and provided local data that was highly representative of the effects of changing test conditions and injector designs. The local data correlated well with the global performance data under every test condition and configuration, and indicated that small rocket behavior was highly dependent upon operating conditions, small changes in injector design, and changes in fuel film cooling rates.

The degree of azimuthal symmetry was found to be dependent upon operating conditions for both injectors. This finding may prove critical to the development of accurate rocket flow field models and requires further investigation to quantify the dependence of injector azimuthal performance upon operating condition.

The global and local data showed that the two injectors had distinctly different performance characteristics with 60% FFC. Because the only known difference between the injectors was a small modification to the upstream region, the results indicate that small differences with injector designs may lead to large differences in performance.

The effects of varying the fuel film cooling rates were evaluated by comparing the data trends with 60% and 75% FFC for both injectors. The two injectors performed similarly with 75% FFC, and exhibited the same trends with nearly identical temperature measurements. However, with 60% FFC the data trends were different than what was observed with 75% FFC. This indicates that the rocket flow field may be dominated by the effects of the fuel film cooling rate at 75% FFC.

The thruster diagnostics were capable of providing local data which were representative of rocket flow field processes. The observed dependency of azimuthal behavior upon operating condition, the performance differences due to small changes in injector designs, and the significant effects due to changes in fuel film cooling may prove important to the design and modeling of small rockets. Although the thruster diagnostics did not provide quantitative flow field parameter data, they identify areas which greatly affected the small rocket operation. Further investigation of these areas may result in the development of more accurate small rocket models and yield improved low thrust rocket designs.

Acknowledgments

The authors wish to acknowledge the efforts of Roger D. Scheman for the fabrication of the thruster water cooling system and support for the testing of the thruster, and of Edward J. Pluta, Stephen H. Culler, William M Furfaro and Pablo A. Gutierrez for electronic support during the hot fire tests. The authors wish to recognize Robert S. Dorrance, Walter E. Hendricks, Patrick Spanos, and Walter A. Wozniak who were intimately involved with the thruster fabrication, and the efforts of Richard Czentorycki which enhanced this work.

References

1. Smith, T.A., "Boundary Layer Development as a Function of Chamber Pressure in the NASA Lewis 1030:1 Area Ratio Rocket Nozzle," AIAA Paper 88-3301, July, 1988.

2. Kehtarnavaz, H. and Coats, D. E., "Thick Boundary Layer Assessment for Nozzle Flow," AIAA Paper 88-3160, July, 1988.

3. Richter, G.P. and Price, H.G., "Proven, Long Life Hydrogen/Oxygen Thrust Chambers for Space Station Propulsion," 1986 JANNAF Propulsion Meeting, August 1986, NASA TM-88822.

4. Smith, T. A., Pavli, A. J., and Kacynski, K.J., "Comparison of Theoretical and Experimental Thrust Performance of a 1030:1 Area Ratio Rocket Nozzle at a Chamber Pressure of 2413 kN/m^2 (350 psia)", NASA TP-2725, 1987.

5. "JANNAF Rocket Engine Performance Prediction and Calculation Manual", CPIA Publication 246, April 1975.

6. Nickerson, G.R., Coats, D.E., and Dang, L.D., Engineering and Programming Manual: "Two Dimensional Kinetic Reference Computer Program (TDK)" NASA CR-178628, Software Engineering Associates, Inc., 1985.

7. Kim, S.C. and Van Overbeke, T. J., "Calculations of Gaseous Hydrogen/Oxygen Thrusters," AIAA Paper 90-2490, July, 1990.

8. Reed, B.D., Penko, P.F., Schneider, S.J., and Kim, S.C., "Experimental and Analytical Comparisons of Flowfields in a 110 N (25 lb_f) H2/O2 Rocket," AIAA Paper 91-2283.

9. Weiss, J. M.and Merkle, C. L., "Numerical Investigation of Reacting Flowfields in Low Thrust Rocket Engine Combustors," AIAA Paper 91-2080, June 1991.

10. Seasholtz, R.G., Zupanc, F.J., and Schneider, S.J., "Spectrally Resolved Rayleigh Scattering Diagnostic for Hydrogen-Oxygen Rocket Plume Studies," *Journal of Propulsion and Power*, **8**, 935-942, 1992.

11. Zupanc, F.J. and Weiss, J.M., "Rocket Plume Flowfield Characterization Using Laser Rayleigh Scattering," AIAA Paper 92-3351, July 1992.

12. de Groot, W.A. and Weiss, J.M., "Species and Temperature Measurement in H2/O2 Rocket Flow Fields by Means of Raman Scattering Diagnostics," NASA CR 189217, AIAA Paper 92-3353, July 1992.

13. Reed, B.D.,"Small Hydrogen/Oxygen Rocket Flowfield Behavior From Heat Flux Measurements," AIAA Paper 93-2162, June, 1993.

14. Schoenman, L. and Block, P.,"Laminar Boundary-Layer Heat Transfer in Low-Thrust Rocket Nozzles," *Journal of Spacecraft*, Vol. 5, No. 9, 1082-1089, 1968.

15. Back, L.H., Cuffel, R.F., and Massier, P.F., "Laminarization of a Turbulent Boundary Layer in Nozzle Flow - Boundary Layer and Heat Transfer Measurements With Wall Cooling," *Journal of Heat Transfer*, 333-344, August 1970.

16. Kacynski, K.J., Pavli, A.J., and Smith, T.A.,"Experimental Evaluation of Heat Transfer on a 1030:1 Area Ratio Rocket," NASA TP-2726, 1987.

17. Rousar, D.C. and Ewen, R.L., "Combustion Effects on Film Cooling,"NASA CR-135052, Aerojet Liquid Rocket Company, February, 1977.

18. Robinson, P.J. "Space Station Auxiliary Thrust Chamber Technology," Final Report, NASA CR-185296, Aerojet Techsystems Company, July 1990.

19. Arrington, L.A. and Reed, B.D.,"Performance Comparison of Axisymmetric and Three-Dimensional Hydrogen Film Coolant Injection in a 110 N Hydrogen/Oxygen Rocket," AIAA Paper 92-3390, July 1992.

20. Arrington, L.A., and Schneider, S.J., "Low Thrust Rocket Test Facility," AIAA Paper 90-2503, July, 1990.

21. Reed, B.D., Penko, P.F., Schneider, S.J., and Kim, S.C.,"Experimental and Analytical Comparision of Flowfields in a 110N(25lbf) H_2/O_2 Rocket," AIAA Paper 91-2283, June 1991.

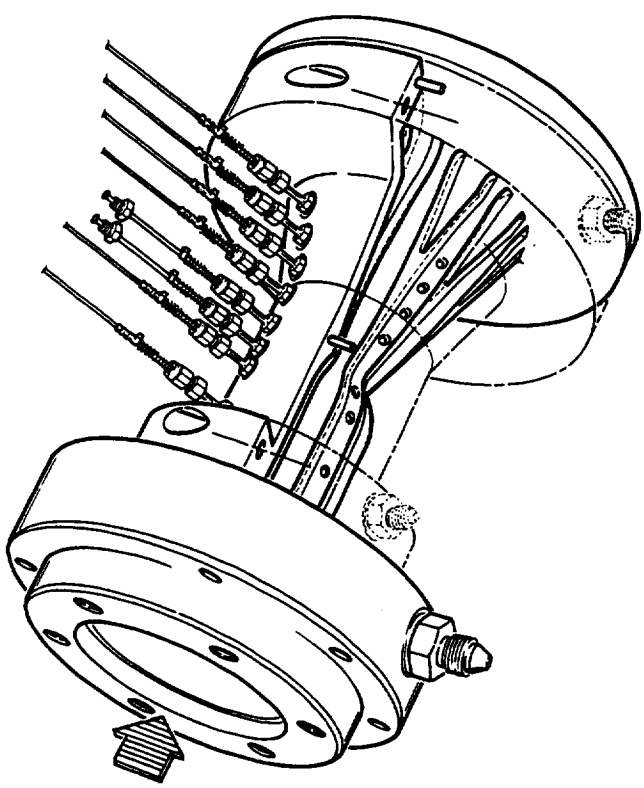

(a) Laboratory thruster instrumentation section.

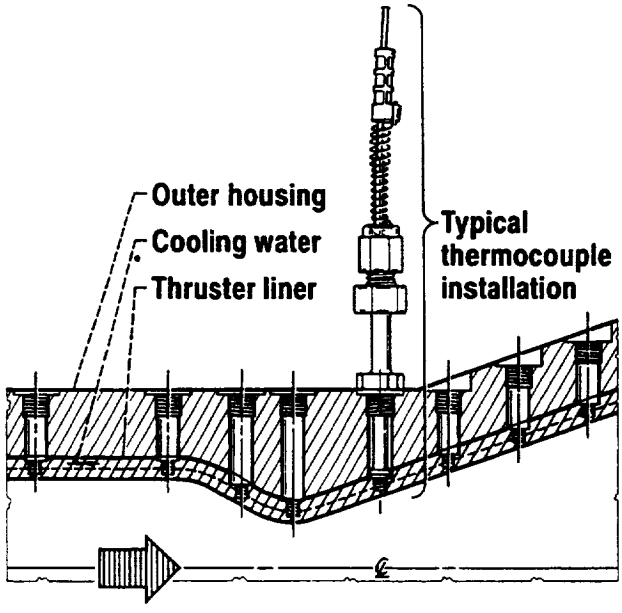

(b) Laboratory thruster instrumentation port details.

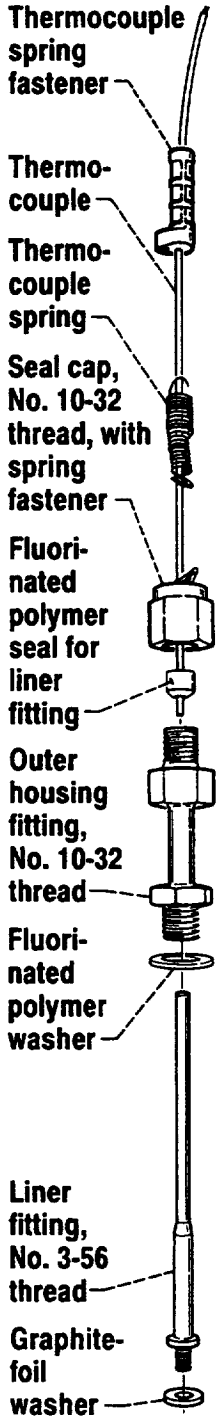

(c) Exploded view of a thermocouple installation.

Figure 1.—Laboratory thruster instrumentation details.

CD-93-63916

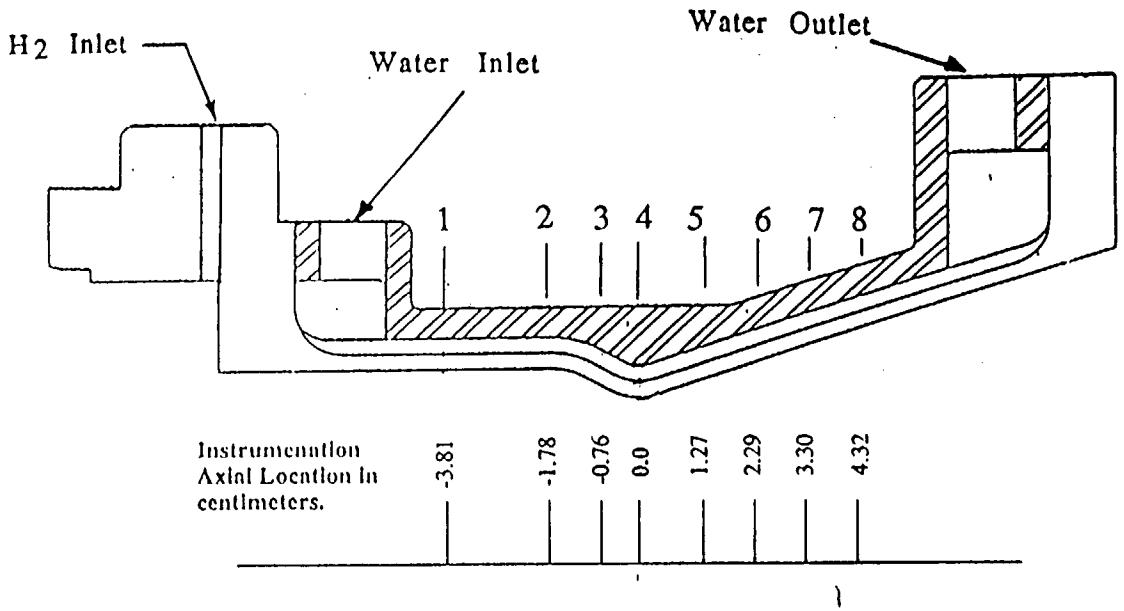

Injector End View of Azimuthal Instrument Location

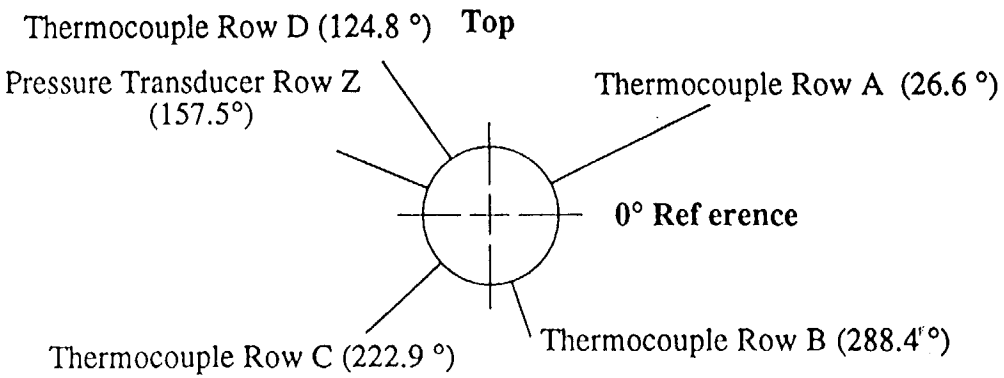

Row	Thermocouple	Pressure Tranducer
A	A1, A2,A3, A5,A6,A7,A8	
B	B1-B8	
C	C1,C2,C3, C5,C6,C7,C8	
D	D1-D8	
Z		Z1,Z2,Z3, Z5,Z6,Z7,Z8

Figure 2. Laboratory Thruster Instrumentation Locations

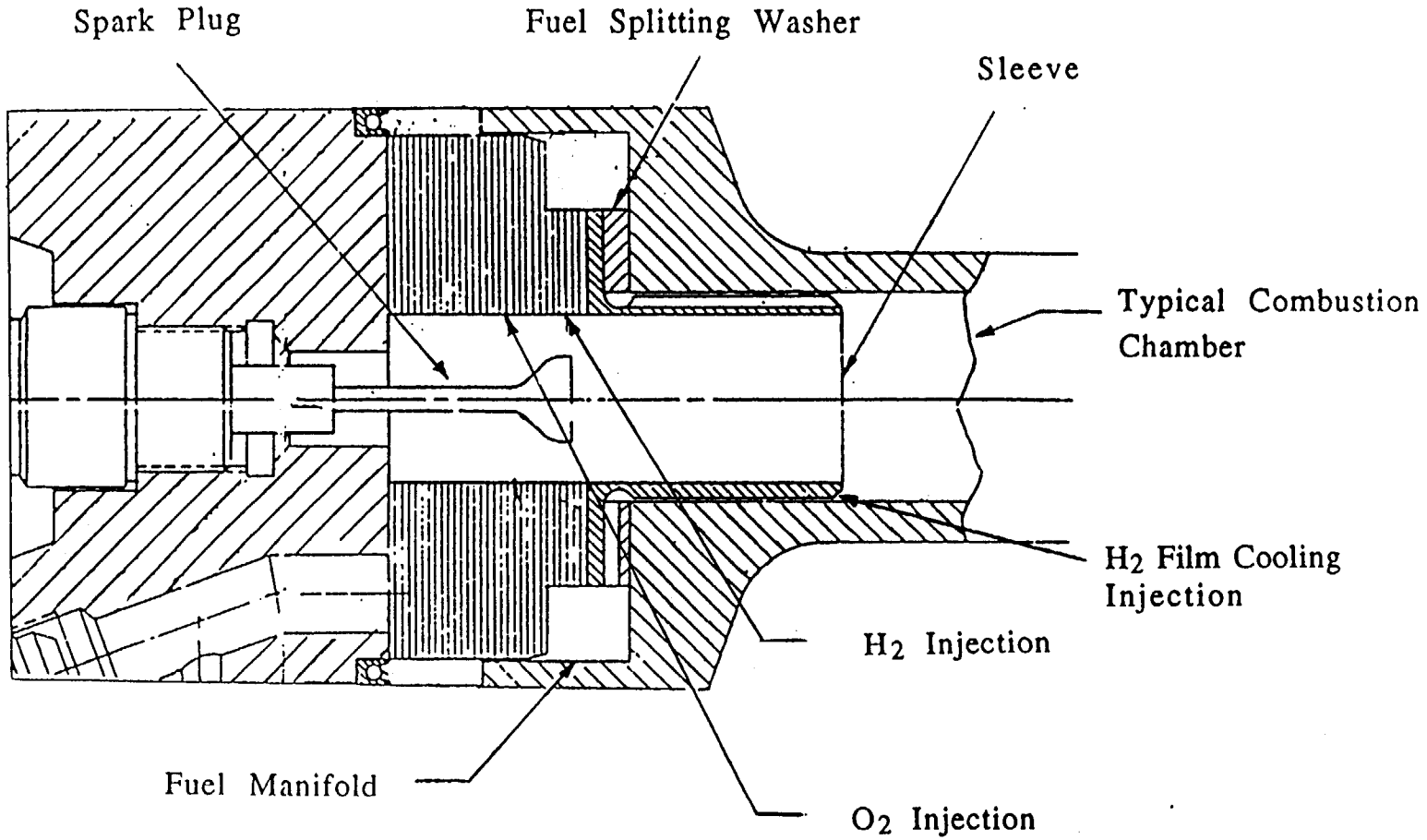

Figure 3. Injector Details for Aerojet SN. 02 and SN. 03 Injectors.

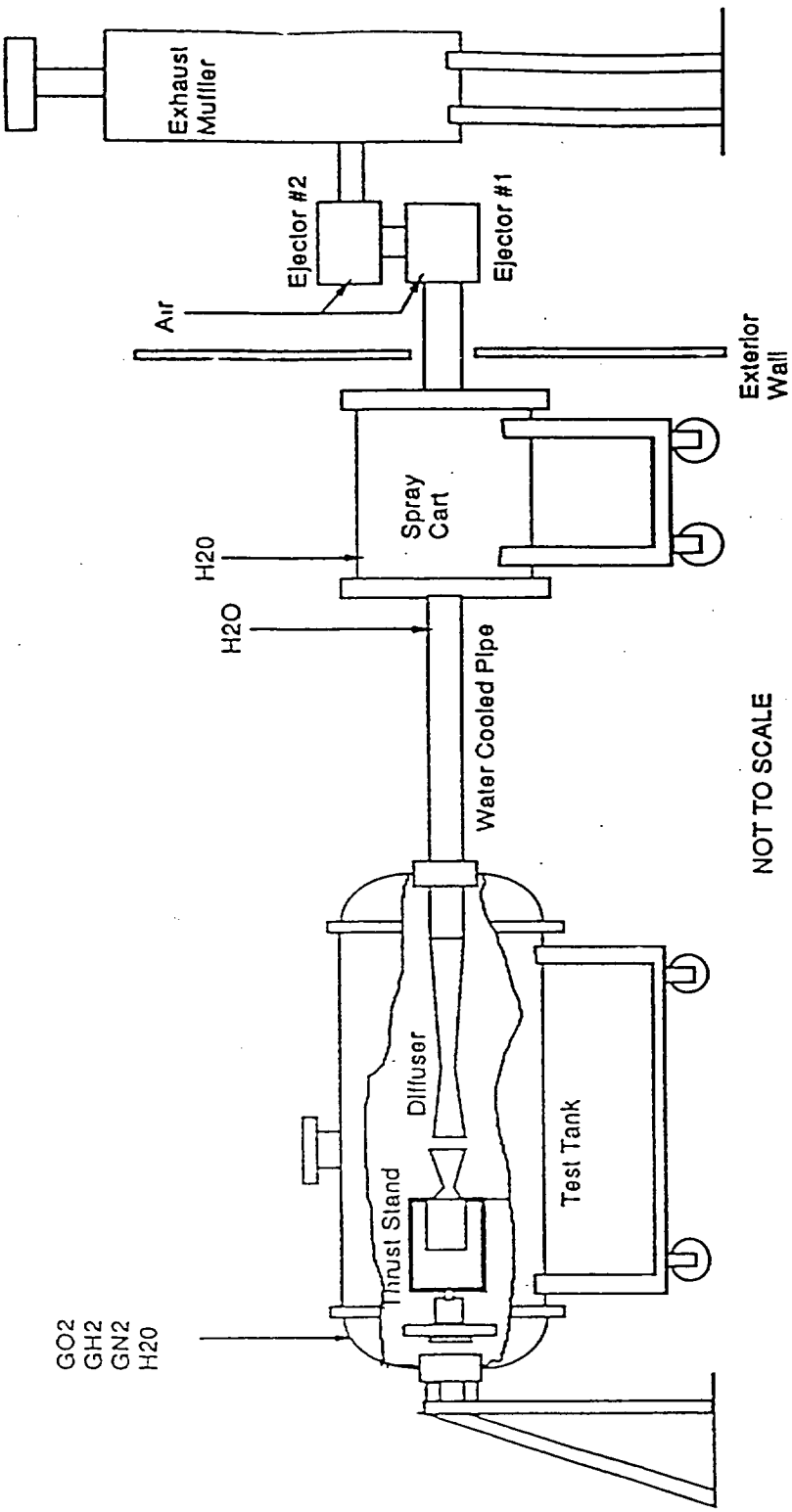

Figure 4. NASA Lewis Research Center RL-11 Test Cell

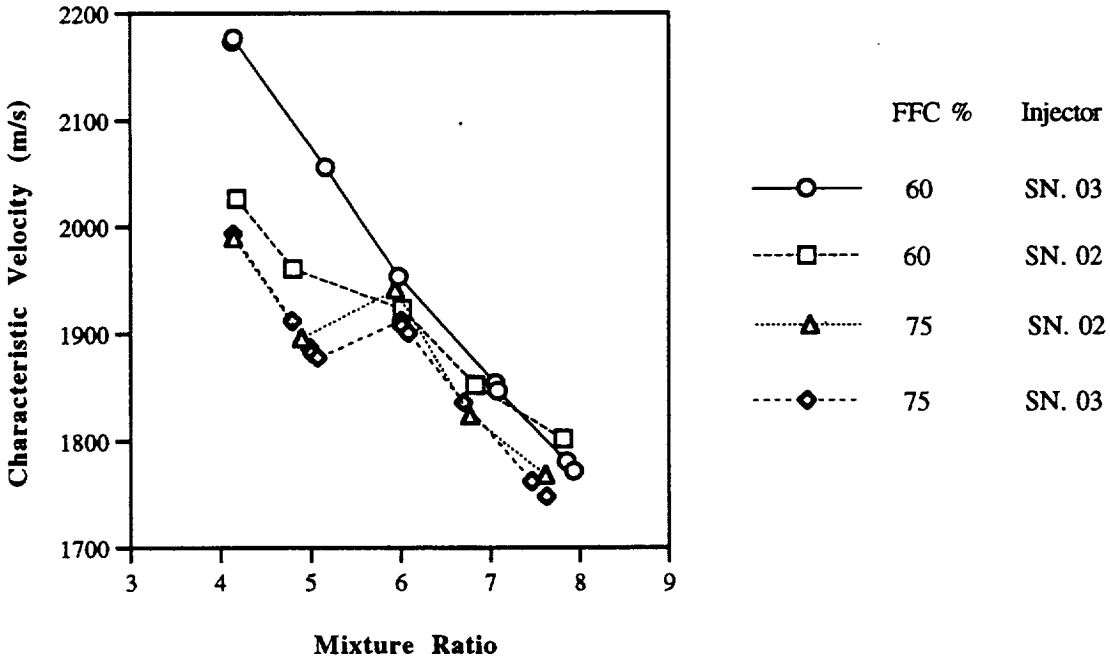

Figure 5. Characteristic Velocity Profiles.
Nominal 500 kPa Chamber Pressure.

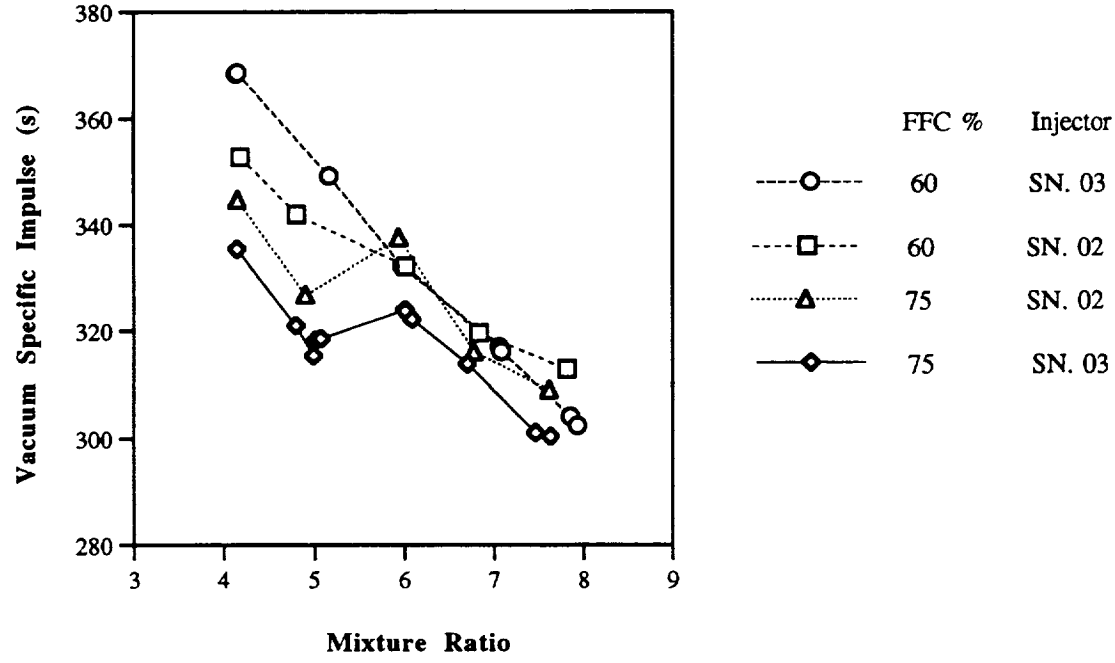

Figure 6. Vacuum Specific Impulse Profiles.
Nominal 500 kPa Chamber Pressure.

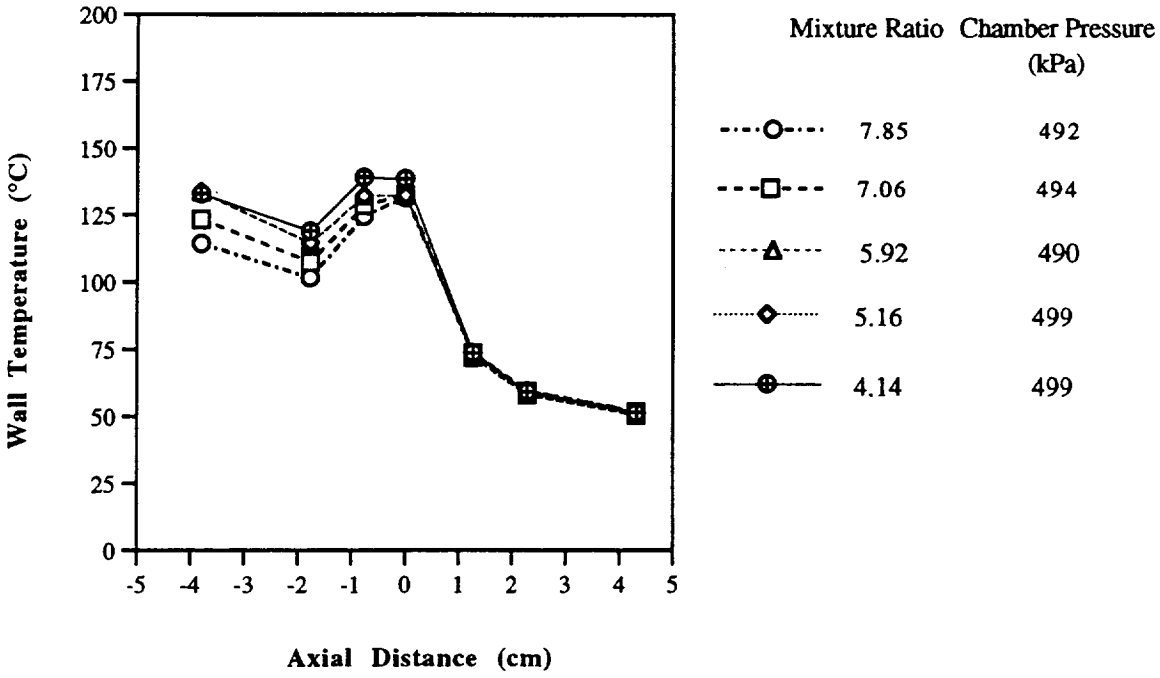

Figure 7. Row B Thermocouple Temperature Profiles.
Injector SN. 03 Thruster Assembly.
Nominal 60% Fuel Film Cooling.

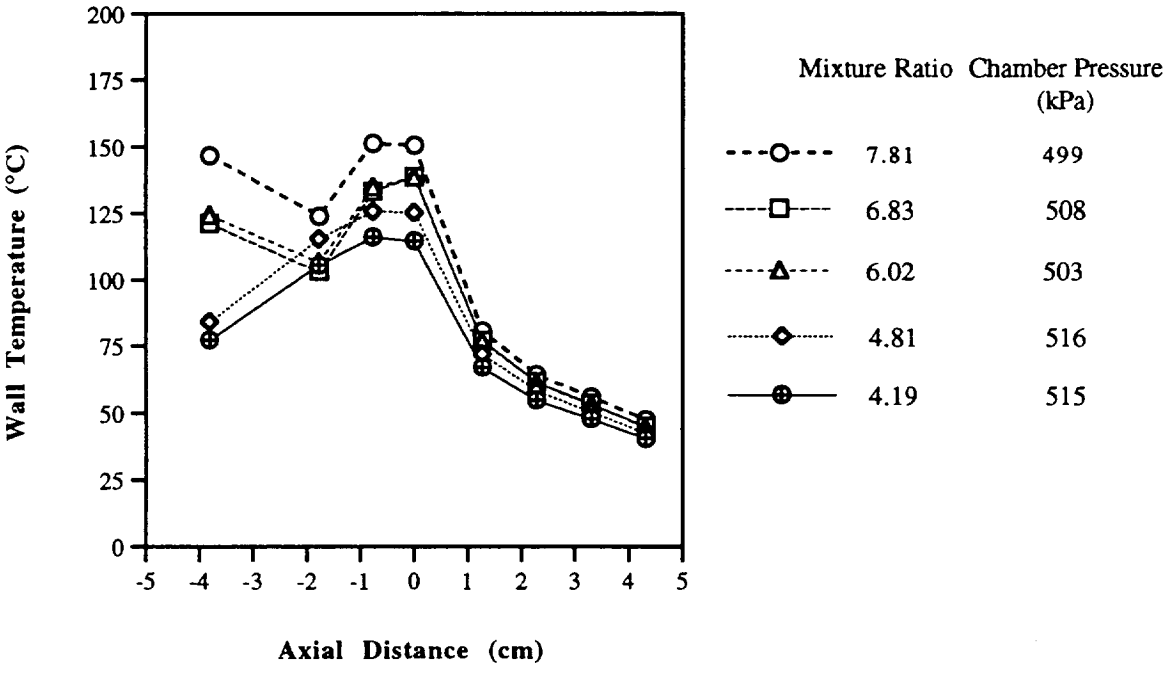

Figure 8. Row B Thermocouple Temperature Profiles.
Injector SN. 02 Thruster Assembly.
Nominal 60% Fuel Film Cooling.

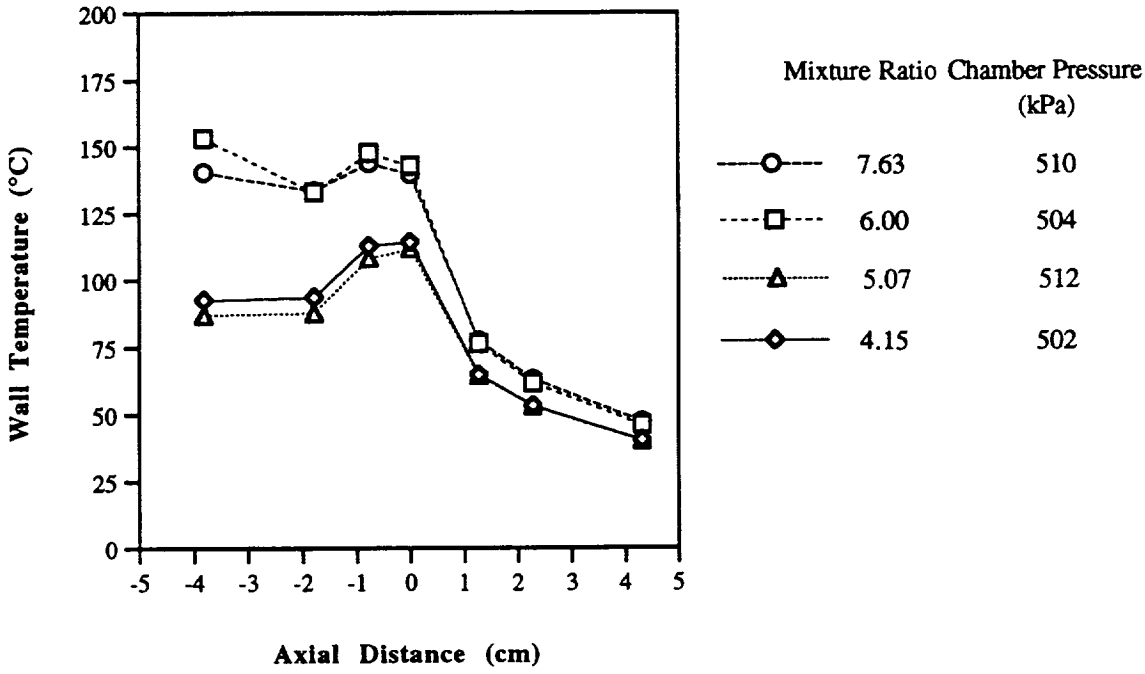

Figure 9. Row B Thermocouple Temperature Profiles.
Injector SN. 03 Thruster Assembly.
Nominal 75% Fuel Film Cooling.

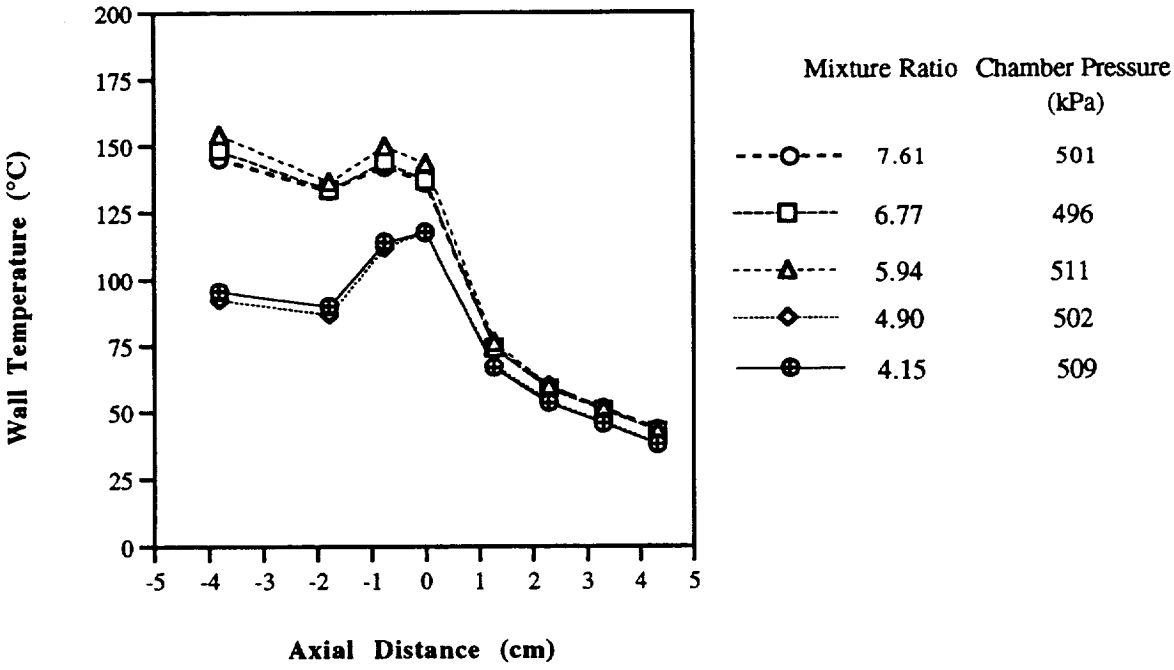

Figure 10. Row B Thermocouple Temperature Profiles
Injector SN. 02 Thruster Assembly.
Nominal 75% Fuel Film Cooling.

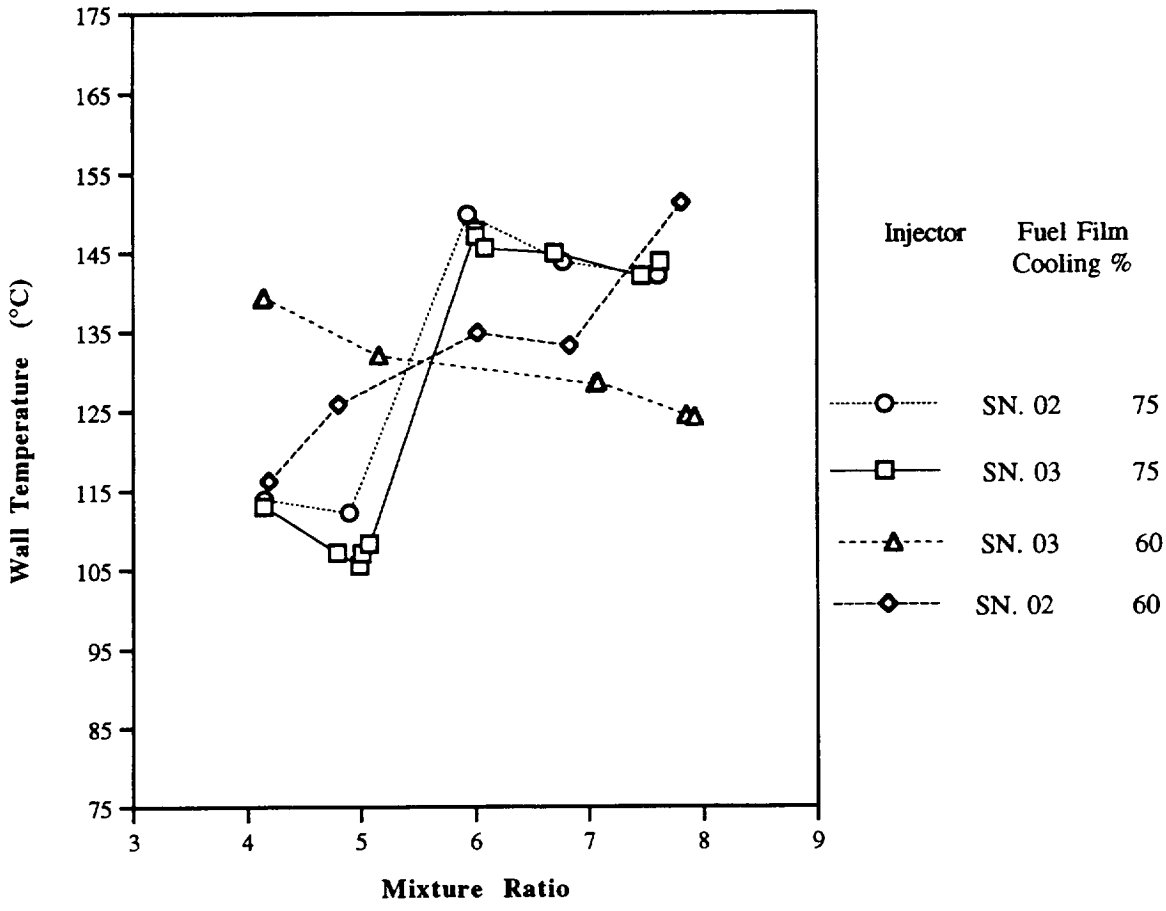

Figure 11. Temperature Profiles at Thermocouple Location B3.
Nominal 500 kPa Chamber Pressure.

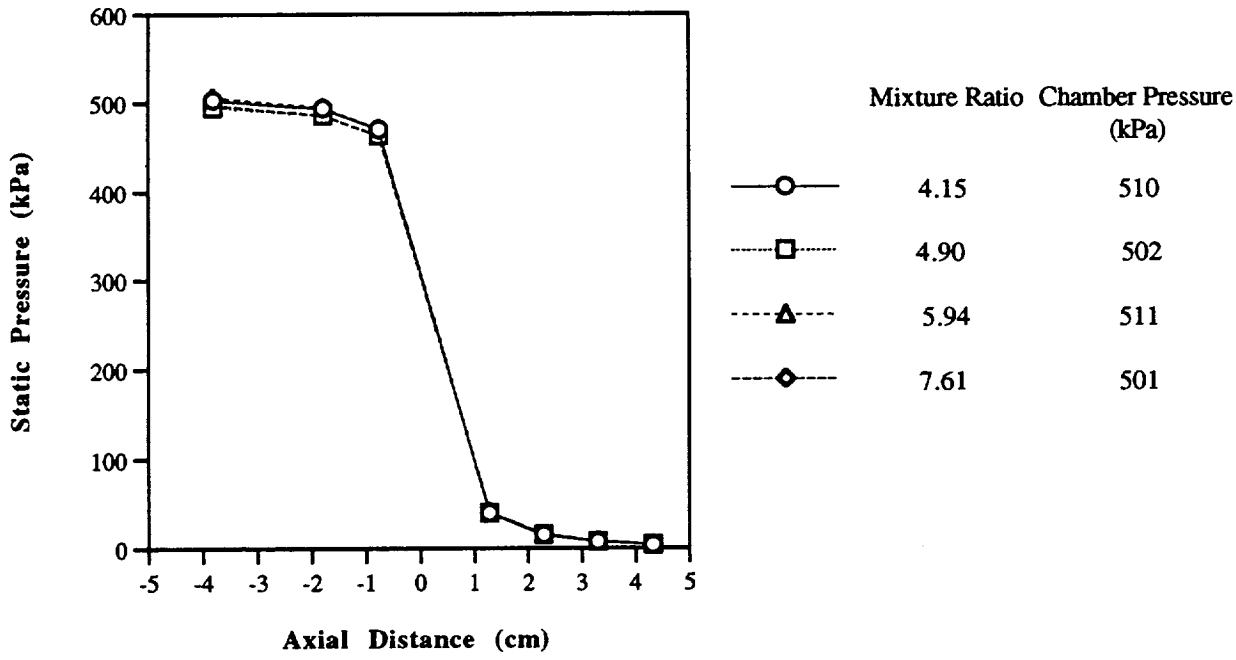

(a) 75% Fuel Film Cooling.

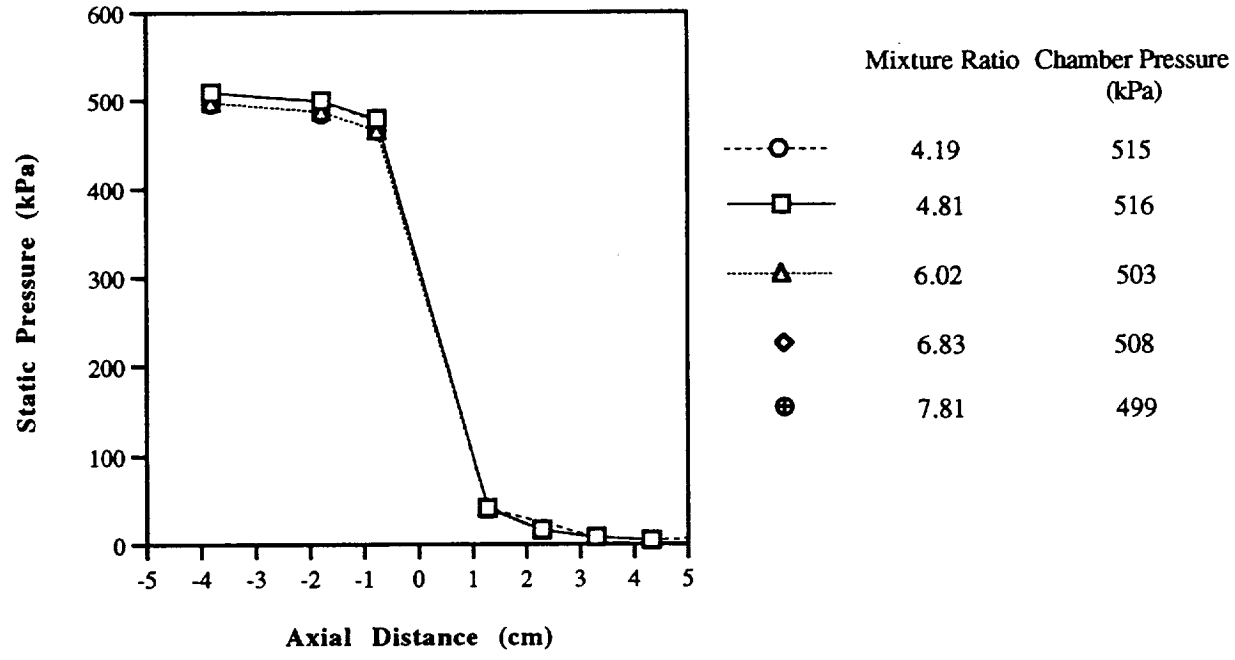

(b) 60% Fuel Film Cooling.

Figure 12. Static Pressure Profiles.
Injector SN. 02 Thruster Assembly.

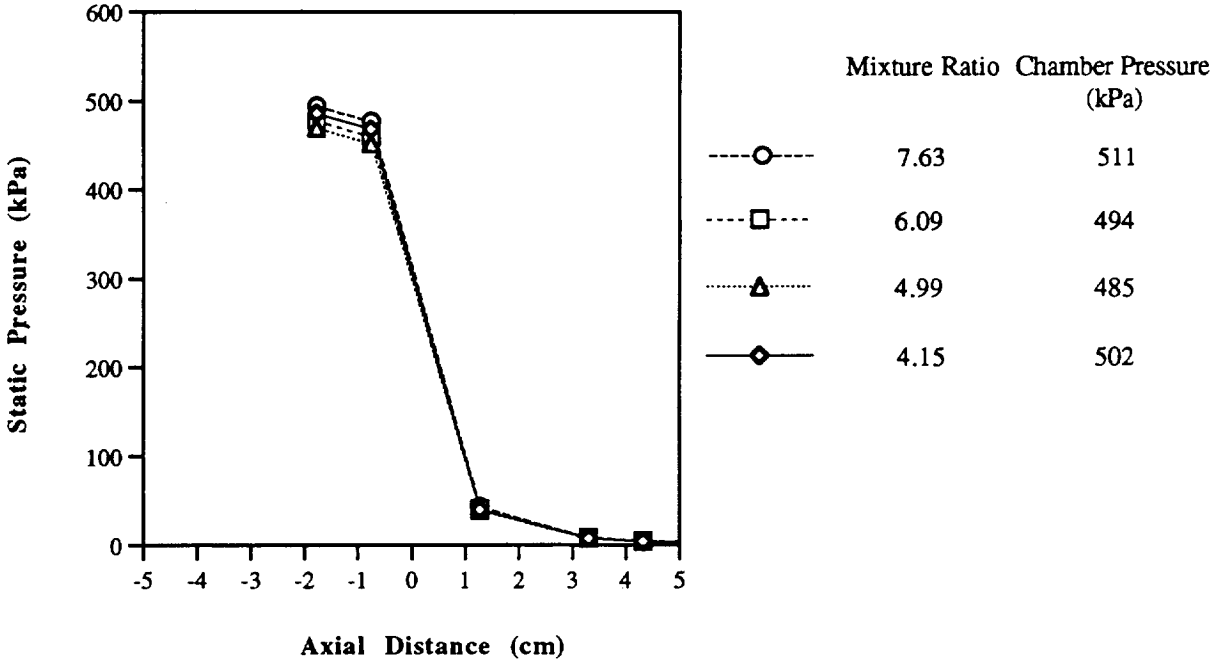

(a) 75% Fuel Film Cooling.

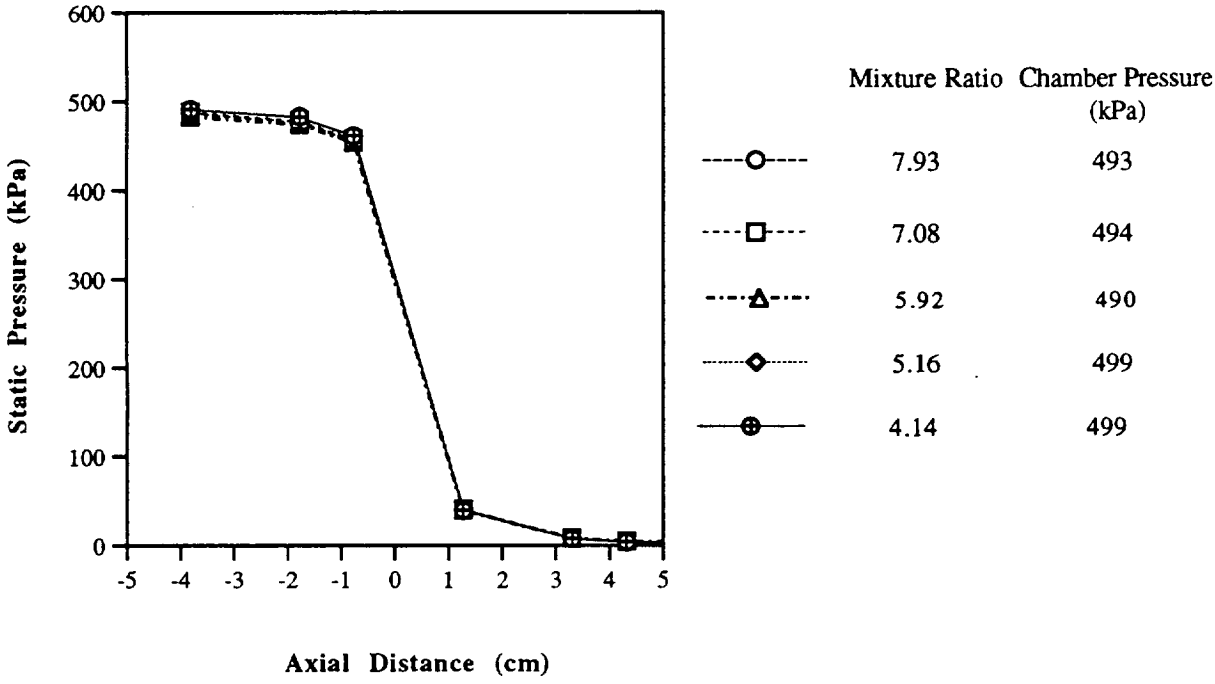

(b) 60% Fuel Film Cooling.

Figure 13. Static Pressure Profiles.
Injector SN. 03 Thruster Assembly.

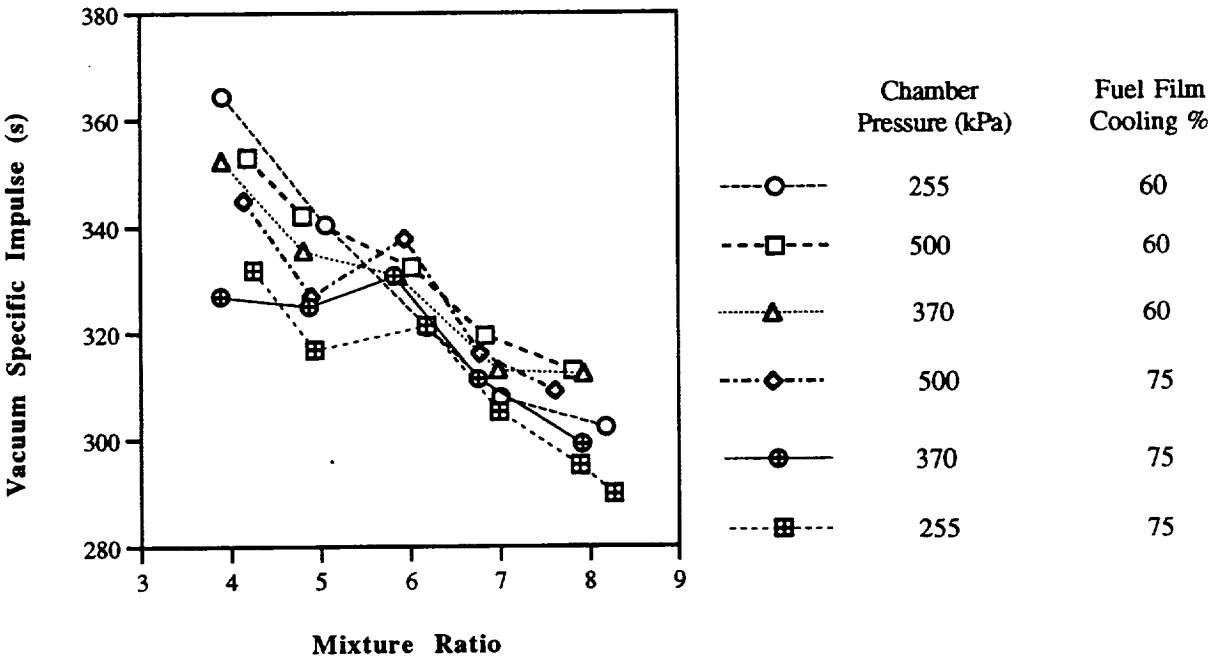

Figure 14. Vacuum Specific Impulse Profiles.
Injector SN. 02 Thruster Assembly.

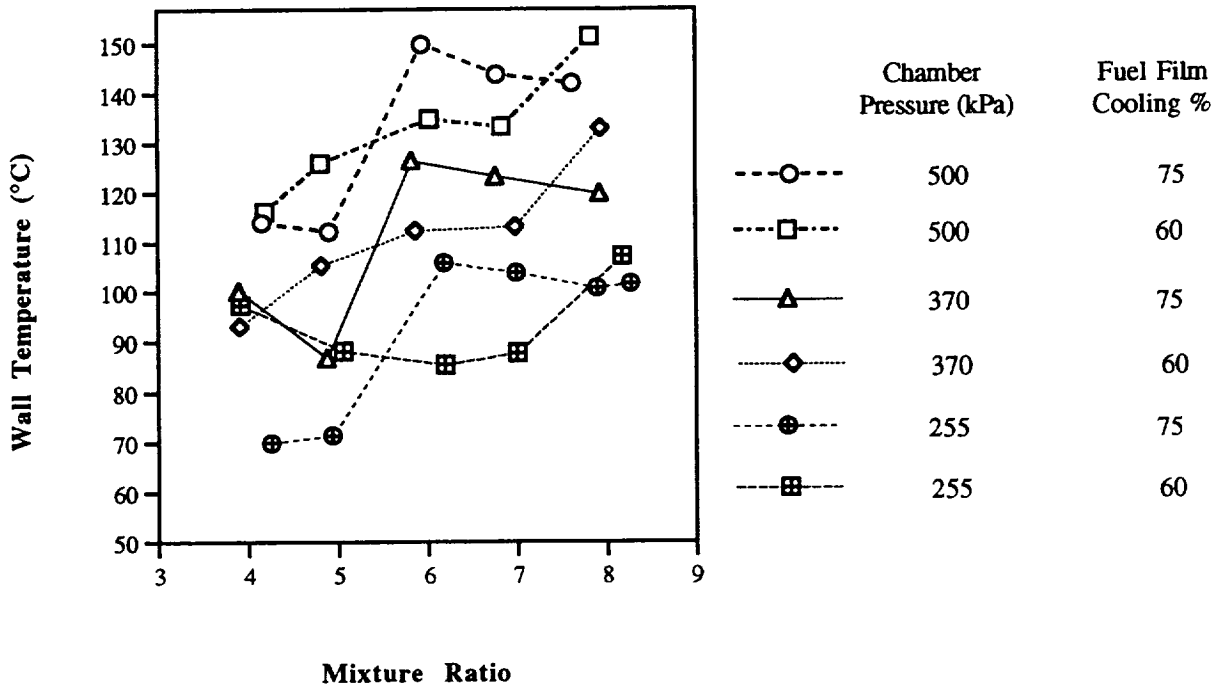

Figure 15. Temperature Profiles at Thermocouple Location B3.
Injector SN. 02 Thruster Assembly.

Appendix A

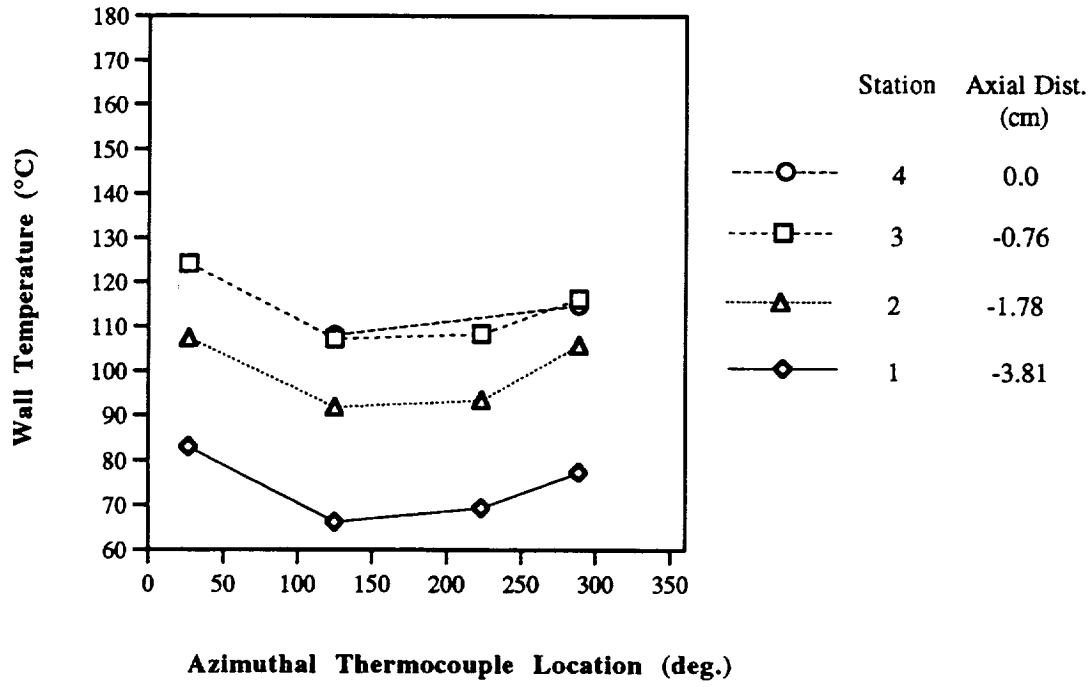

(a) 4.19 Mixture Ratio.
515 kPa Chamber Pressure.

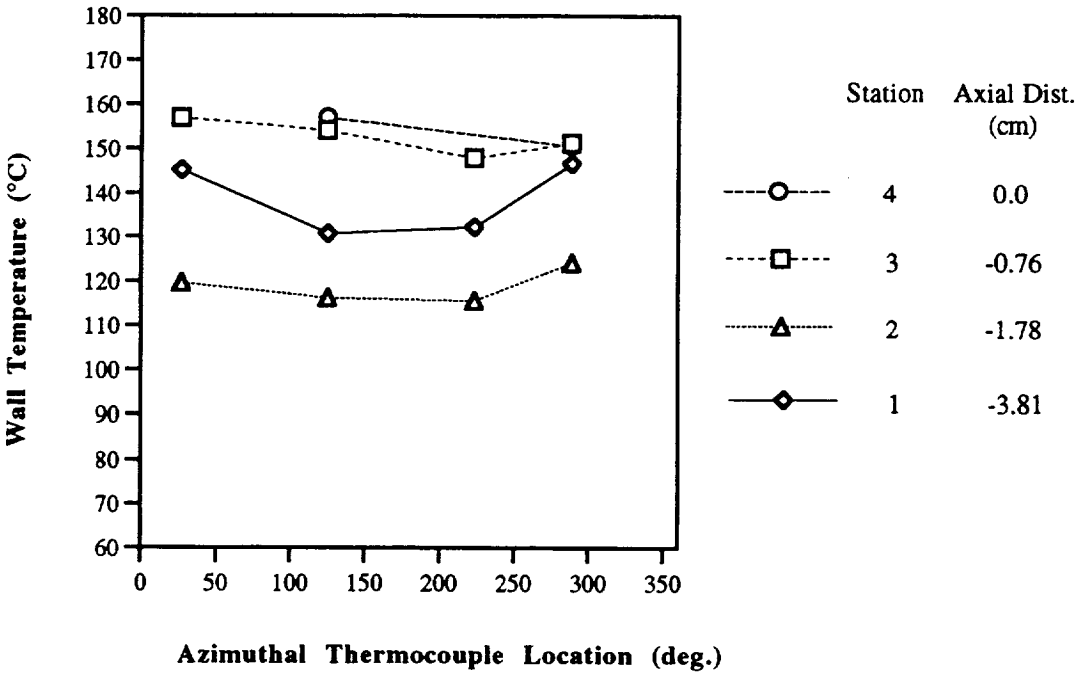

(b) 7.81 Mixture Ratio.
499 kPa Chamber Pressure.

Figure A1. Azimuthal Temperature Profiles.
Injector: SN. 02 Thruster Assembly.
Nominal 60% Fuel Film Cooling.

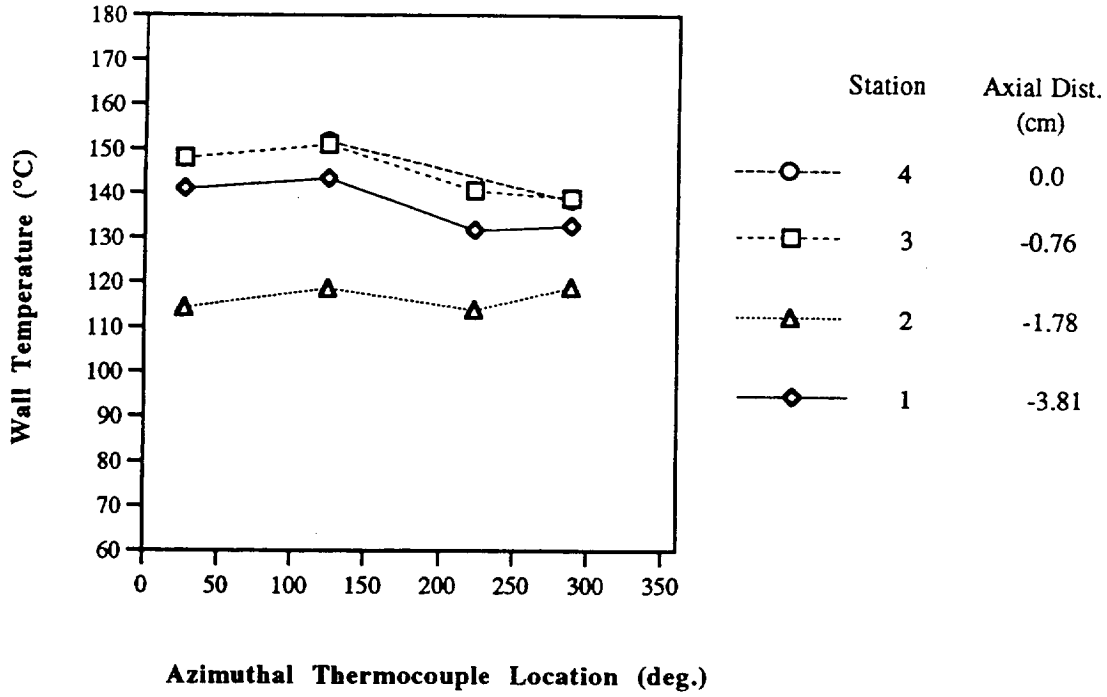

(a) 4.14 Mixture Ratio.
499 kPa Chamber Pressure.

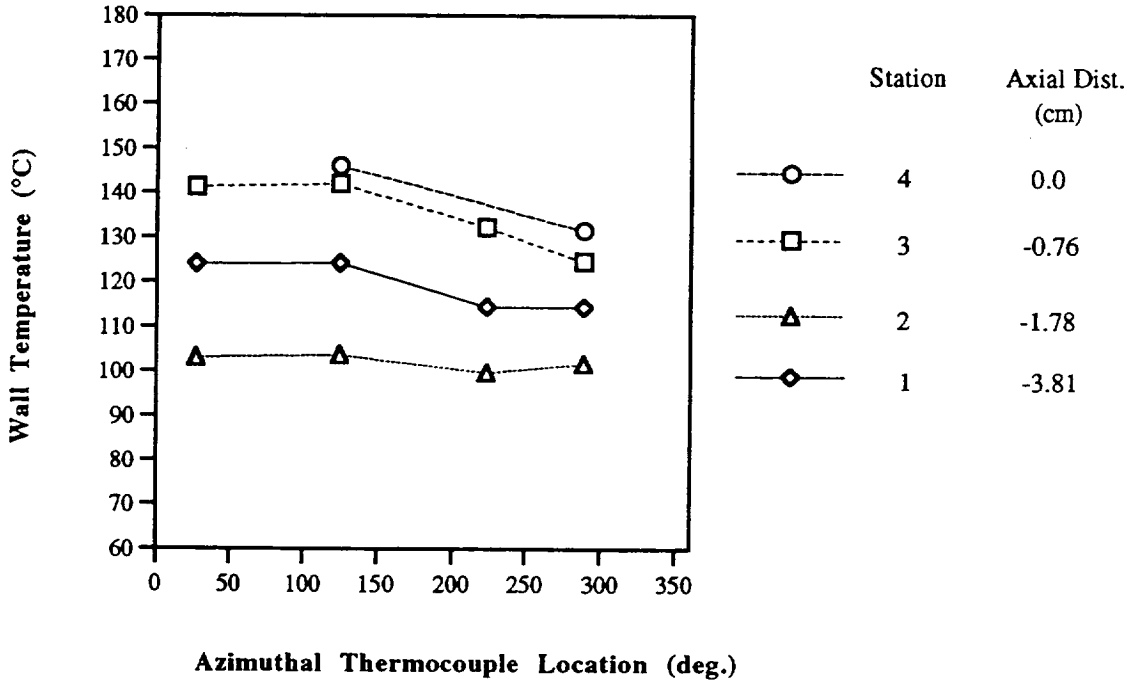

(b) 7.85 Mixuture Ratio.
492 kPa Chamber Pressure.

Figure A2. Azimuthal Temperature Profiles.
Injector: SN. 03 Thruster Assembly.
Nominal 60% Fuel film Cooling.

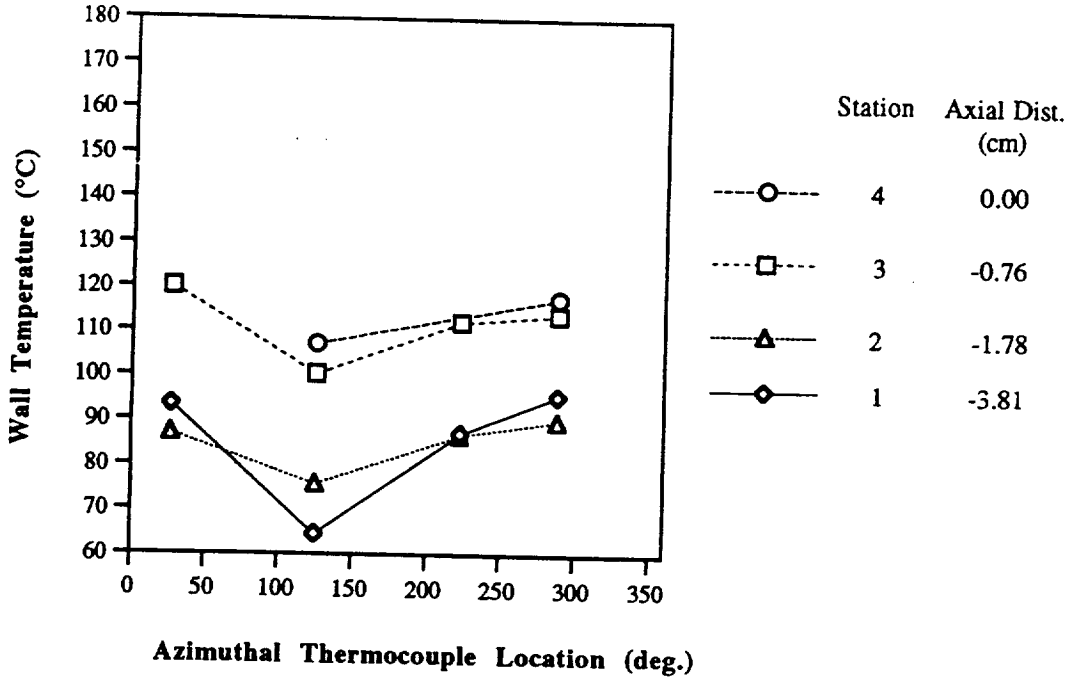

(a) 4.15 Mixture Ratio.
510 kPa Chamber Pressure.

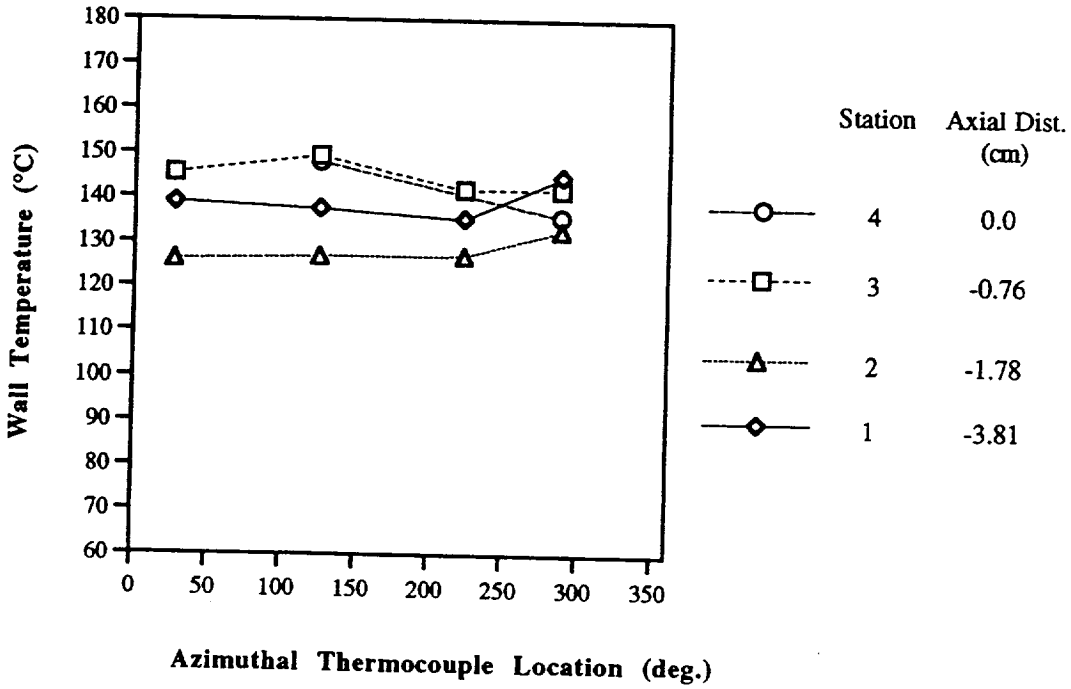

(b) 7.61 Mixture Ratio.
501 kPa Chamber Pressure.

Figure A3. Azimuthal Temperature Profiles.
Injector: SN. 02 Thruster Assembly.
Nominal 75% Fuel Film Cooling.

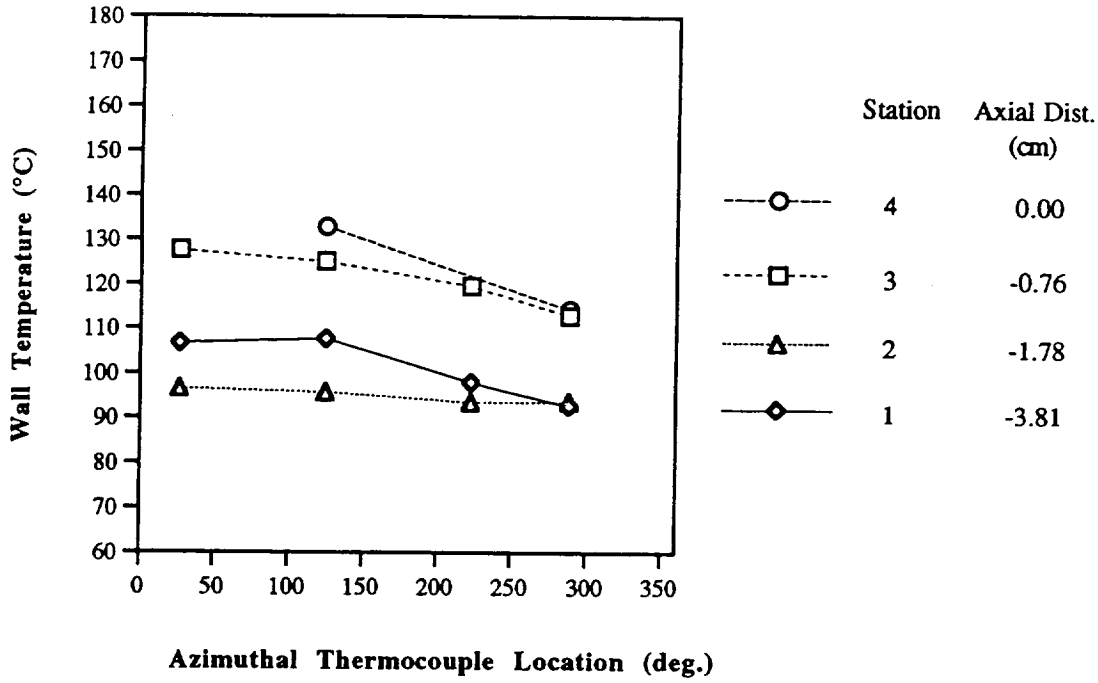

(a) 4.15 Mixture Ratio.
502 kPa Chamber Pressure.

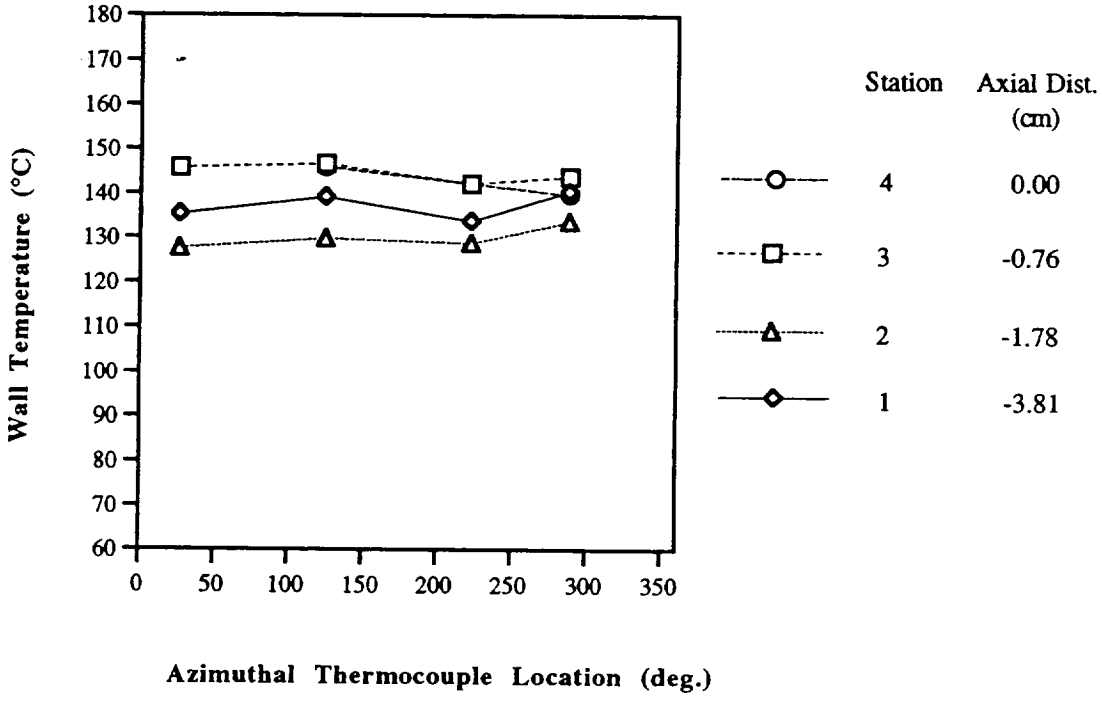

(b) 7.63 Mixture Ratio.
511 kPa Chamber Pressure.

Figure A4. Azimuthal Temperature Profiles.
Injector: SN. 03 Thruter Assembly.
Nominal 75% Fuel Film Cooling.

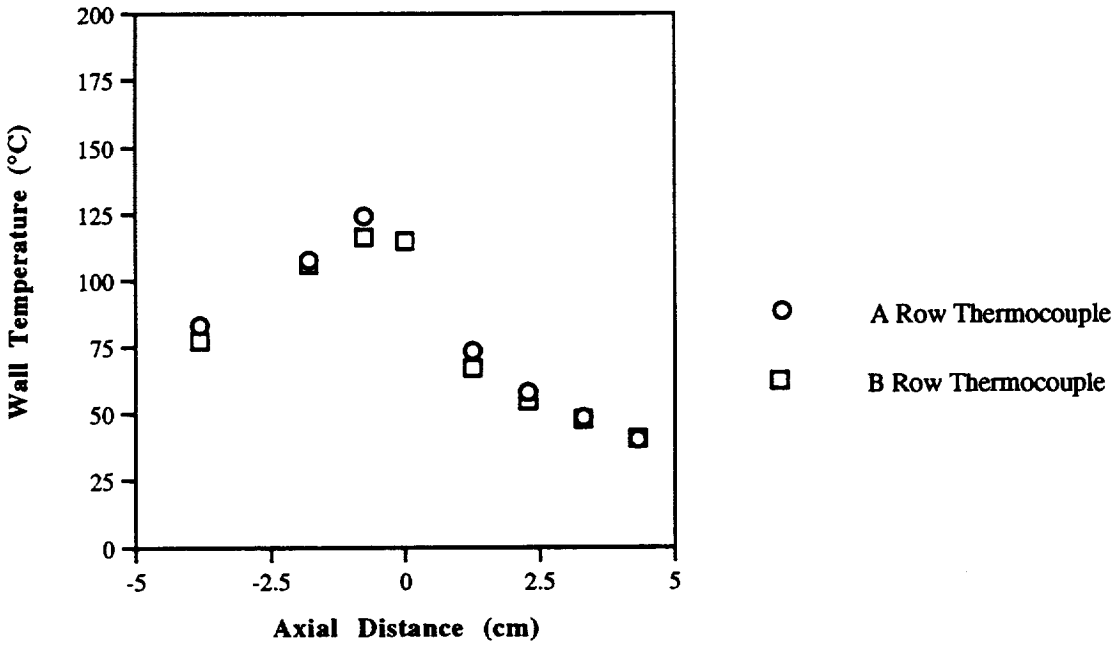

(a) Nominal 60% Fuel Film Cooling at Mixture Ratio of 4.19.

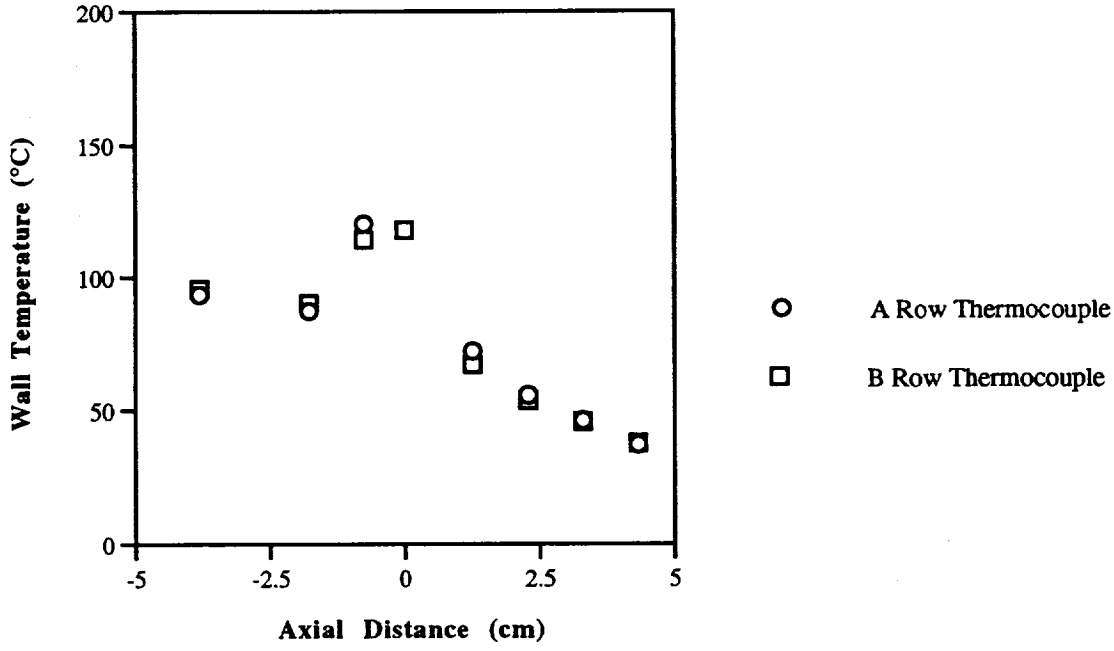

(b) Nominal 75% Fuel Film Cooling at Mixture Ratio of 4.15.

Figure A5. Temperature Profiles for Thermocouple Rows A, and B.
Injector SN. 02 Thruster Assembly.
Nominal 500 kPa Chamber Pressure.

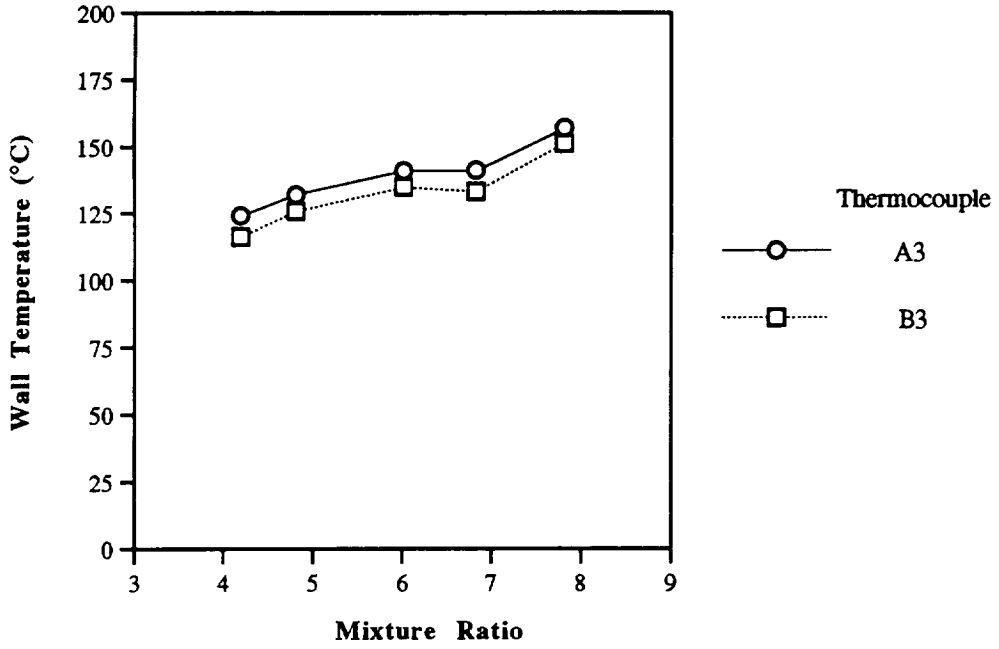

(a) Nominal 60% Fuel Film Cooling.

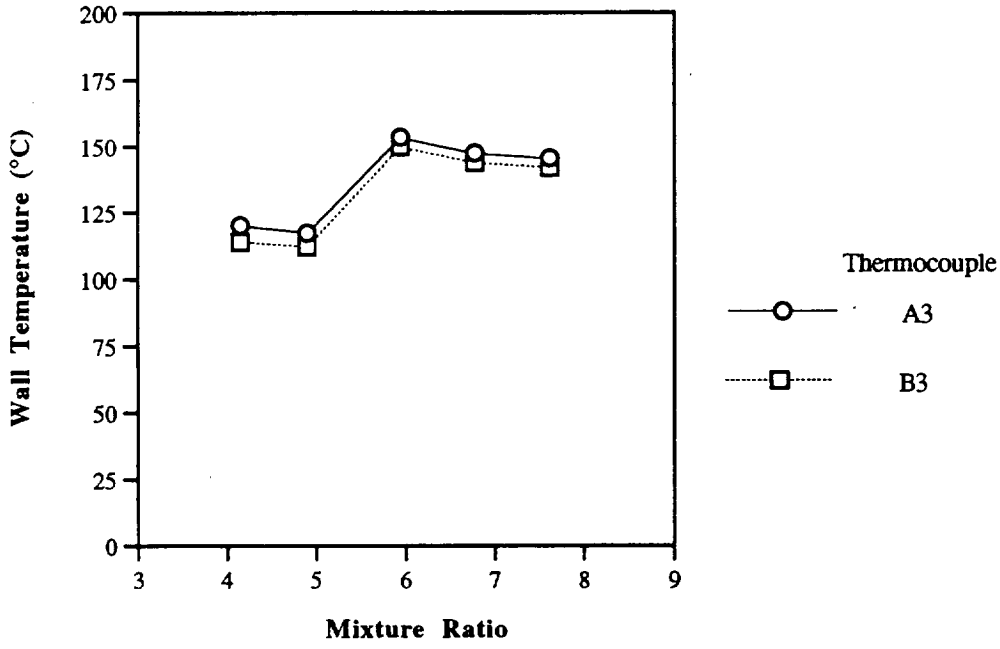

(b) Nominal 75% Fuel Film Cooling.

Figure A6. Temperature Profiles for Thermocouple Location A3, and B3.
Injector SN. 02 Thruster Assembly.
Nominal 500 kPa Chamber Pressure.

REPORT DOCUMENTATION PAGE

Form Approved
OMB No. 0704-0188

1. AGENCY USE ONLY (*Leave blank*)	2. REPORT DATE	3. REPORT TYPE AND DATES COVERED
	June 1993	Technical Memorandum

4. TITLE AND SUBTITLE

A Laboratory Model of a Hydrogen/Oxygen Engine for Combustion and Nozzle Studies

5. FUNDING NUMBERS

WU-506-42-31

6. AUTHOR(S)

Sybil Huang Morren, Roger M. Myers, Stephen E. Benko, Lynn A. Arrington, and Brian D. Reed

7. PERFORMING ORGANIZATION NAME(S) AND ADDRESS(ES)

National Aeronautics and Space Administration
Lewis Research Center
Cleveland, Ohio 44135-3191

8. PERFORMING ORGANIZATION REPORT NUMBER

E-7813

9. SPONSORING/MONITORING AGENCY NAME(S) AND ADDRESS(ES)

National Aeronautics and Space Administration
Washington, D.C. 20546-0001

10. SPONSORING/MONITORING AGENCY REPORT NUMBER

NASA TM-106281
AIAA-93-1825

11. SUPPLEMENTARY NOTES

Prepared for the 29th Joint Propulsion Conference and Exhibit sponsored by the AIAA, SAE, ASME, and ASEE, Monterey, Calinfornia, June 28-30, 1993. Sybil Huang Morren, NASA Lewis Research Center; Roger M. Myers, Sverdrup Technology, Inc., Lewis Research Center Group, 2001 Aerospace Parkway, Brook Park, Ohio 44142; Stephen E. Benko, NASA Lewis Research Center; Lynn A. Arrington, Sverdrup Technology, Inc., 2001 Aerospace Parkway, Brook Park, Ohio 44142; and Brian D. Reed, NASA Lewis Research Center. Responsible person, Sybil Huang Morren, (216) 433-7482.

12a. DISTRIBUTION/AVAILABILITY STATEMENT

Unclassified - Unlimited
Subject Category 20

12b. DISTRIBUTION CODE

13. ABSTRACT (*Maximum 200 words*)

A small laboratory diagnostic thruster was developed to augment present low thrust chemical rocket optical and heat flux diagnostics at the NASA Lewis Research Center. The objective of this work was to evaluate approaches for the use of temperature and pressure sensors for the investigation of low thrust rocket flow fields. The nominal engine thrust was 110 N. Tests were performed at chamber pressures of about 255 kPa, 370 kPa, and 500 kPa with oxidizer to fuel mixture ratios between 4.0 and 8.0. Two gaseous hydrogen/gaseous oxygen injector designs were tested with 60% and 75% fuel film cooling. The thruster and instrumentation designs were proven to be effective via hot fire testing. The thruster diagnostics provided inner wall temperature and static pressure measurements which were compared to the thruster global performance data. For several operating conditions, the performance data exhibited unexpected trends which were correlated with changes in the axial wall temperature distribution. Azimuthal temperature distributions were found to be a function of operating conditions and hardware configuration. The static pressure profiles showed that no severe pressure gradients were present in the rocket. The results indicated that small differences in injector design can result in dramatically different thruster performance and wall temperature behavior, but that these injector effects may be overshadowed by operating at a high fuel film cooling rate.

14. SUBJECT TERMS

H/O engine; Hot fire tested

15. NUMBER OF PAGES
34

16. PRICE CODE
A03

17. SECURITY CLASSIFICATION OF REPORT	18. SECURITY CLASSIFICATION OF THIS PAGE	19. SECURITY CLASSIFICATION OF ABSTRACT	20. LIMITATION OF ABSTRACT
Unclassified	Unclassified	Unclassified	